UNIVERSITY OF CALIFORNIA SAN DIEGO

2-Nitrofuran Arylamide Compounds as Innate Immune Modulators

A Thesis submitted in partial satisfaction of the requirements for the degree
Master of Science

in

Biology

by

Yuya Fujita

Committee in charge:

Professor Mary P. Corr, Chair
Professor Stephen M. Hedrick, Co-Chair
Professor Elina I. Zuniga

2019

The Thesis of Yuya Fujita is approved, and is acceptable in quality and form for publication on microfilm and electronically:

_____

_____

Co-Chair

_____

Chair

University of California, San Diego

2019

TABLE OF CONTENTS

LIST OF ABBREVIATIONS

BMDC = Bone Marrow-Derived Dendritic Cells

DEXA = Dexamethasone

DMSO = Dimethylsulfoxide

DMXAA = Xanthenone Analog a.k.a Vadimezan or ASA404

ELISA = Enzyme-Linked Immunosorbent Assay

FRET = Fluorescence Resonance Energy Transfer

GPI = Glucose-6 Phosphate Isomerase

HTS = High-Throughput Screening

IC_{50} = Half Maximal Inhibitory Concentration

IFN = Interferon

IL = Interleukin

IP = Intraperitoneal

IP10 = Interferon Gamma-Induced Protein 10

IRF = Interferon Regulatory Factor

IT = Intrathecal Treatment

LPS = Lipopolysaccharide

MTT = 3-(4,5-dimethylthiazol-2-yl)-2,5-diphenyltetrazolium bromide

MyD88 - Myeloid Differentiation Primary Response 88

N.D. = Not Dectected

NF-κB = Nuclear Factor Kappa B

ODN = Oligodeoxynucleotides

PBS = Phosphate-Buffered Saline

Poly I:C = Polyinosinic:Polycytidylic Acid

R-INH = Repurchased Inhibitor

RA = Rheumatoid Arthritis

SAR = Structure Activity Relationship

SD = Standard Deviation

SEM = Standard Error of the Mean

STING = Stimulator of Interferon Genes

TLR = Toll-like Receptor

TNF = Tumor Necrosis Factor

TRIF - TIR-Domain-Containing Adapter-Inducing Interferon-β

UTC = 5-(4-fluorophenyl)-2-ureido-thiophene-3 carboxylic acid amide

WT = Wild Type

LIST OF FIGURES

LIST OF TABLES

ACKNOWLEDGEMENTS

I would like to acknowledge Dr. Mary P. Corr for her support as the chair of my committee. Her guidance over the years has proved to be invaluable.

I would like to acknowledge the members of the Corr and Carson labs for their help and support.

I would also like to acknowledge Dr. Stephen M. Hedrick and Dr. Elina I. Zuniga for serving as members of my committee and contributing their time to support my thesis.

I would also like to acknowledge Dr. Michelle Arkin at University of California San Francisco for providing the chemical library used in the screening project of this thesis.

Section 3.1 Role of TLR4 in Allodynia and Cytokine Expression, in part, is a reprint of the material as it appears in Neuraxial TNF and IFN-beta co-modulate persistent allodynia in arthritic mice 2018. Woller, Sarah A.; Ocheltree, Cody; Wong, Stephanie Y.; Bui, Anthony; Fujita, Yuya; Gonçalves dos Santos, Gilson; Yaksh, Tony Y.; Corr, Maripat, Brain, Behvavior, and Immunity, 2018. The thesis author was a co-author of this paper.

This thesis, in part, is currently being prepared for submission for publication of the material. Fujita, Yuya; Hosoya, Tadashi; Shukla, Nikunj; Cottam, Howard; Hayashi, Tomoko; Carson, Dennis; Corr, Mary P. The thesis author was the primary investigator and author of this material.

ABSTRACT OF THE THESIS

2-Nitrofuran Arylamide Compounds as Innate Immune Modulators

by

Yuya Fujita

Master of Science in Biology

University of California San Diego, 2019

Professor Mary P. Corr, Chair
Professor Stephen M. Hedrick, Co-Chair

Autoimmune diseases such as rheumatoid arthritis affect millions of patients and many of these diseases have yet to find a cure. Transcription factors like nuclear factor-κB (NF-κB) play an important role in chronic inflammatory diseases. While previously investigated as a drug target, NF-κB inhibitors have failed due to adverse effects observed in clinical studies likely due to impairment of cellular homeostasis and increased toxicity resulting from complete NF-κB inhibition. We aimed to identify immunosuppressant

compounds by reanalyzing data from a prior high-throughput screen using a cell-based NF-κB reporter assay in human monocytic THP-1 cells with a 166,304 compound library. Candidate compounds were screened for suppression of LPS-induced NF-κB activity. We identified 270 hit compounds through a naïve “Top X” approach. These compounds were further analyzed for their effects on cellular viability and cytokine production in human and murine cell lines. Compounds from the 2-nitrofuran arylamide compounds reduced TNFα, IFNβ, and IP10 effectively when ligands for TLR3, TLR7, TLR9, and STING were used as a primary stimulus. In a preliminary study, treatment with two of these compounds prevented the onset of allodynia, but do not change swelling in a K/BxN mouse model. Further analysis of these compounds and this chemical family may yield potential drug therapies to treat patients afflicted with autoimmune disorders associated with the overproduction of innate cytokines.

1 Introduction

1.1 Rheumatoid Arthritis

Rheumatoid arthritis (RA) is a chronic autoimmune disease distinguished by joint inflammation and cartilage destruction resulting from autoantibodies circulating in the body that target various endogenous molecules (Smolen et al. 2018). Autoantibodies, such rheumatoid factor (RF) directed against the Fc region of immunoglobulin G, have been associated with RA, but individuals with RA have been identified without these autoantibodies (Smolen et al. 2018). Increased expression of pro-inflammatory cytokines including interleukin-1 (IL-1), interleukin 6 (IL-6), and tumor necrosis factor alpha (TNFα) that contribute to arthritic swelling is another pathological characteristic which has been associated with RA and other autoimmune diseases (Scott et al., 2010).

While understanding of the molecular mechanisms of arthritic inflammation has been increasingly studied over the recent decades, the exact cause of RA has not been fully elucidated, and a multitude of factors such as genetic disposition and receptor disorders are suspected to be involved in the manifestation of this disease. Studies of disease concordance among monozygotic twins have revealed a three times higher prevalence of RA when compared to dizygotic twins, showing that genetics does affect susceptibility to RA (D. M. Lee and Weinblatt 2001). However, many other environmental factors such as smoking are contributing factors to the disease as they can result in oxidative stress and apoptosis in immune cells that can stimulate the onset of autoimmune disorders (Chang et al., 2014).

In addition to environmental and genetic factors, the sex of an individual has been implicated as an influencer of RA. Similar to other autoimmune diseases, RA has been observed at a three times higher rate in women than in men and has partly been associated with stimulatory effects of the estrogen hormone on the immune system (Smolen et al. 2018). Female patients with arthritic disorders are more likely to report worse pain and symptoms than males with RA (Woller et al., 2018).

Joint pain is one of the primary reasons why RA patients seek medical attention (Borenstein et al. 2010). Psychological and emotional distress stemming from chronic pain has been connected to fatigue and a lower quality of life in RA patients (Minnock et al., 2015; Murphy et al., 2012). However, pain resulting from RA often persists despite treatment to resolve inflammation of the joints. The underlying mechanisms of pain and sex differences in RA need to be further studied to develop better remission treatments of arthritic pain.

Several different classes of RA treatments are currently available including disease modifying anti-rheumatic drugs (DMARDs), glucocorticoids, immunosuppressants, non-steroidal anti-inflammatory drugs (NSAIDs), and biological response modifiers (Burmester et al., 2017). However, these treatments only help to alleviate the symptoms of RA and do not cure the disease. As a treatment to permanently cure RA has not yet been discovered, patients require constant treatment for the remainder of their lives to abate the symptoms.

Furthermore, some of the current treatments like DMARDs can cause side effects such as ulcers, gastrointestinal discomfort, and hepatotoxicity

(Wilsdon et al., 2017). Glucocorticoid treatments of RA can also cause patients to experience osteoporosis, high blood pressure, cataracts, and weight gain when taken for prolonged periods of time (Yeap et al., 2002). The method of administration for some newer treatments is also difficult to ensure adherence from patients as some, such as biologics, require daily self-injection by the patient (Curtis et al., 2013). Therefore, it is important that new treatments are developed with diminished side effects and easier routes of administration. Potential new treatments may involve small-molecules that target the activity of certain transcription factors and adaptor proteins like NF-κB and interferon regulator factors that have been associated with autoimmune diseases.

1.2 The K/BxN Murine Model of Arthritis

The complex nature of rheumatoid arthritis has necessitated the development of appropriate animal models of RA to investigate causes of the disease and potential treatments. The K/BxN model involves the cross-breeding of KRN mice, which contain transgenic genes encoding a T-cell receptor, with non-obese diabetic (NOD) mice (Kouskoff et al. 1996). The cross-breeding of KRN mice on a C57BL/6 background (K/B mice) with NOD mice generates K/BxN offspring whose serum can be transferred to recipient mice to induce transient inflammatory arthritis (Kouskoff et al. 1996). Inflammatory arthritis is induced through the autoantibodies in the serum of the K/BxN mice which are specific against glucose-6-phosphate isomerase (GPI), which is arrayed on the surface of joint cartilage (Matsumoto et al., 1999). The K/BxN model causes transient paw inflammation and robust mechanical allodynia, or

central pain sensitization, in male C57BL/6 serum-recipient mice (Christianson et al., 2010, 2012). Male C57BL/6 mice also develop arthritis but do not recover from their pain following resolution of swelling which highlights the differences of disease pathology between sexes (Christianson et al. 2012).

The development of the passive K/BxN serum transfer model of arthritis has allowed for better assessment of the mechanisms of RA pathogenesis. The model creates a predictable onset of arthritis in recipient mice through the injection of equal quantities of autoantibodies against GPI. Following the serum transfer, the induced arthritis typically resolves over time as antibodies are cleared without replacement in the serum-injected mice which allows for better normalization between experiments (Christianson et al. 2012). Recipient mice of the K/BxN serum develop mechanical allodynia together with inflammation of the joints and paws which is characteristic of RA in human patients. Cytokines, like type I interferons and interleukins, and immune structures, including Toll-like receptors (TLRs), are involved in modulating RA progression (Corr et al., 2011; Corr et al., 2009). These cytokines and structures have been implicated in facilitating the progression of RA and investigation on how to modify these targets may serve to treat the disease.

1.3 Type I Interferons

Interferons (IFNs) serve a major role in antiviral immunity through interactions with various cells of the host immune system and are one of the main cytokine groups involved in RA (Corr et al. 2009). IFNs are produced by most major cell types and function to modulate the immune system to better

counter viral infections (González-Navajas et al., 2012). There are three main classes of interferons: type I, type II, and type III. Of these three classes, type I IFNs are the largest family and bind to the IFN-α/β receptor. Within the type I IFN family, interferon-alpha (IFN-α) and interferon-beta (IFN-β) are well characterized in their various roles in the immune system including stimulating leukocytes such as macrophages and NK cells to secrete other cytokines (Mcnab et al., 2015). Once surface or intracellular binding to receptors such as TLRs or RIG-I (retinoic acid-inducible gene I) occurs, activation of transcription factors like interferon regulator factor (IRF) 3 and IRF7 results in type I interferon production.

Studies of rheumatoid arthritis have shown that type I interferons can play several roles in the disease. As neuropathic pain is centralized, treatment directly in the spinal cord, or intrathecal treatment (IT), may serve to alleviate pain caused by RA. To determine the differences in pain development in WT and *Tlr4*$^{-/-}$, we investigated the behavior of cytokines over time in respective arthritis mouse models. Through analysis of samples harvested from these mice, we found differences in how certain cytokines are upregulated and downregulated in these mice when given arthritis (Woller et al. 2018).

To translate these findings, we demonstrated that a treatment involving co-administration of intrathecal IFN-β and anti-TNF-α antibodies permanently reversed tactile allodynia in male C57BL/6 WT mice (Woller et al., 2018). IFN-β has also been reported to have anti-inflammatory effects through its ability to downregulate TNF-α and IL-1β, resulting in the subsequent production of IL-10, an anti-inflammatory interleukin (van Holten et al,, 2002). From this data, we

believe the identification of drugs which can cause the upregulation of IFN-β and downregulate TNF-α may serve to reduce RA-derived pain. By modulating the expression of type I IFNs, anti-inflammatory cytokines may serve to reduce swelling in the joints of RA patients. Several receptors exist which can initiate the transcription of type I interferons. Among these receptors are the TLRs, the cytosolic RNA sensor RIG-I, the stimulator of interferon genes (STING) adaptor protein, and the DNA-dependent activator of IRF (González-Navajas et al., 2012).

1.4 Toll-like Receptors (TLRs)

Various pathways have been investigated for their association with RA and have been identified as responsible for the production of cytokines involved with the disease. A common mechanism of interferon production involves the cascade pathway associated with Toll-like receptors (TLRs). Toll-like receptors are pattern recognition receptors (PRR) which recognize molecules specifically shared by pathogens but not host molecules. These pathogenic molecules, which are recognized by TLRs, are collectively known as pathogen-associated molecular patterns (PAMPs) and include lipopolysaccharide (LPS) and flagellin (Vaure et al., 2014). TLRs can be broadly categorized into two groups: surface TLRs on the cell membrane and endosomal TLRs on intracellular endosomal compartments (Table 1). Several TLRs have been shown to activate a downstream cascade resulting in the stimulation of interferon production (González-Navajas et al. 2012). Due to their connection to innate immune

pathways that produce pro-inflammatory cytokines, TLRs have been studied to determine their role in the onset of RA.

One TLR which has been gaining attention is Toll-like receptor 4 (TLR4), a surface TLR whose pattern recognition receptor whose primary specificity is for LPS recognition. TLR4 was previously identified as having a key role in the progression of chronic, post-inflammatory allodynia in the murine serum transfer model of arthritis (Christianson et al., 2011). Previous findings of the resolution of pain in male *Tlr4*$^{-/-}$ mice versus chronic pain persistence in male WT mice suggested a connection between TLR4 and the resolution of allodynia (Woller et al. 2018). This finding indicates that pathways associated with TLR4 can be manipulated to alleviate or cure symptoms of autoimmune diseases.

To investigate how TLR4 can be modified to treat RA, it is necessary that both of its pathways are considered for their production of cytokines. Two main pathways are involved in TLR4 signaling: 1) a MyD88 (myeloid differentiation primary response 88)-dependent pathway and 2) a TRIF (TIR-domain-containing adapter-inducing interferon-β)-dependent pathway (Vaure et al., 2014). Once TLR4 binds and recognizes LPS, it can trigger a response through one or both of these pathways to stimulate the production of cytokines to invoke a response against the pathogen. The MyD88-dependent pathway primarily signals the NF-κB complex to regulate the immune system and produce inflammatory cytokines such as TNFα and IL-8. The TRIF-dependent pathway primarily signals through IRF3, which produce type I IFNs. However, the TRIF-dependent pathway also stimulates NF-κB to mediate an induction of pro-inflammatory cytokine genes that worsen RA swelling (Liu et al., 2017).

Table 1. TLR ligands and expression patterns. TLRs are expressed on various innate immune cells and recognize a diverse set of pathogen-associated molecular patterns (Beutler 2019; Kawasaki and Kawai 2014; S. M. Lee et al. 2018).

Receptor	Ligands	Expression	Location
TLR1	Peptidoglycan Triacylated Lipoproteins	B Cells Dendritic Cells Subset Monocytes	Plasma Membrane
TLR2	Glycolipids Lipoproteins Lipoteichoic Acid	Mast Cells Monocytes Myeloid Dendritic Cells	Plasma Membrane
TLR3	Double-stranded RNA Poly I:C	Dendritic Cells B Cells	Endosome
TLR4	LPS	Intestinal Epithelium Monocytes Myeloid Dendritic Cells Mast Cells	Plasma Membrane
TLR5	Flagellin	Dendritic Cell Subset Intestinal Epithelium Monocytes	Plasma Membrane
TLR6	Diacylated Lipopeptides Lipoteichoic Acid	B Cells Mast Cells Monocytes	Plasma Membrane
TLR7	Single-stranded RNA	B Cells Monocytes Plasmacytoid Dendritic Cells	Endosome
TLR8	Single-stranded RNA	B Cells Monocytes Plasmacytoid Dendritic Cells	Endosome
TLR9	CpG DNA	B cells Monocytes Plasmacytoid Dendritic Cells	Endosome
TLR10	dsDNA	B Cells Monocytes Neutrophils	Endosome
TLR11	Flagellin Profilin	Bladder Epithelium Kidney Cells Liver Cells Monocytes	Endosome

1.5 Stimulator of Interferon Genes (STING)

STING is an endoplasmic reticulum-resident transmembrane protein that functions as a cytosolic DNA sensor and as an adaptor protein. It induces the production of type I IFNs production following infection of host cells with viral pathogens. The downstream signaling of STING mainly involves two transcription factors, IRF3 and NF-κB, which promote the production of Type I IFNs and pro-inflammatory cytokines, respectively (Li et al., 2017). Mutations of the STING complex have been shown to cause overproduction of IFNs which subsequently results in autoimmune diseases (Liu et al., 2014). An analysis of samples from patients with systemic inflammation, cutaneous vasculopathy, and pulmonary inflammation revealed that gain of function mutations in STING caused STING-associated vasculopathy with onset in infancy (SAVI), an autoinflammatory disease (Liu et al., 2014). Development of STING antagonists to suppress IFN production may help treat diseases like SAVI and other autoinflammatory diseases such as RA. Similar to the aforementioned STING, the role of the NF-κB transcription factor identifies it a potential target to modulate autoimmune diseases. To identify potential chemical compounds that can suppress the activity of the NF-κB complex, we conducted a screening of a chemical library to discriminate prospective inhibitors.

1.6 High-Throughput Screening (HTS) & Förster Resonance Energy Transfer

High-throughput screening (HTS) is a method used to conduct quick chemical and pharmacological testing of extensive chemical libraries to

discriminate compounds that express desired activity (Hann et al., 2004). Frequently, HTS studies are conducted with the integration of a robotic assay system where robots perform compound treatments on plated cells and collect sample data of specific assays (Oprea 2002). To screen for novel small compounds that express potential immunosuppressant activity of the NF-κB complex to treat autoimmune diseases, we conducted an HTS of a chemical library with a Förster resonance energy transfer (FRET) based CellSensor NF-κB-bla reporter assay in THP-1 cells, a human monocytic leukemic cell line. We used HTS to analyze the initial main chemical library of 166,304 compound for suppression of the NF-κB complex.

Förster resonance energy transfer (FRET) is a technology used to assess the energy transferred between two connected fluorophores, a light-sensitive molecule (Bajar et al., 2016). An initial excitation wavelength directed to a fluorophore passes through the fluorophore and is emitted at a higher wavelength (Figure 1). When two fluorophores are coupled together in a close bond, this emitted wavelength can in turn serve as a secondary excitation wavelength on the second fluorophore (Miyawaki 2011). This wavelength is consequently modified again upon passing through the second fluorophore and is emitted at an even higher wavelength. Due to an inverse proportionality between energy transfer and the distance between donor and acceptor chromophores, FRET assay readings taken are easily influenced by distances between fluorophores (Bajar et al., 2016). Thus FRET assays can determine whether fluorophores are within a certain proximity to one another. For the particular FRET based CellSensor NF-κB-bla reporter in THP-1 cells, NF-κB

induces the production of the beta-lactamase enzyme which breaks the bond between the fluorophores, thus enabling quantification of NF-κB activity through assessment of emission wavelengths from separated fluorophores (Chan et al. 2017).

Following the HTS we performed in this project, a specific group of compounds were identified as potential immunosuppressants. Further testing of these compounds was conducted in both human and murine cell lines to assess cell viability and suppression of LPS induced cytokine secretion following compound treatment. These assays identified several compounds from the 2-Nitro Furan Arylamide chemotype which have similar chemical scaffolds. A previously described covalent small-molecule inhibitor of STING from this chemotype indicated that these compounds are potential STING antagonists (Haag et al. 2018). To test the interactions of the compounds with STING, cellular assays were conducted by treating cells with both the compound candidates and a STING agonist to observe how cytokine production was affected. Assessment of these compounds treated dually with the agonists revealed that they suppressed levels of type I IFNs produced by STING stimulation. Through testing of these compounds in the K/BxN model, we hope to observe decreases in the level of arthritic pain and swelling and test the use of STING antagonists in treating autoimmune diseases.

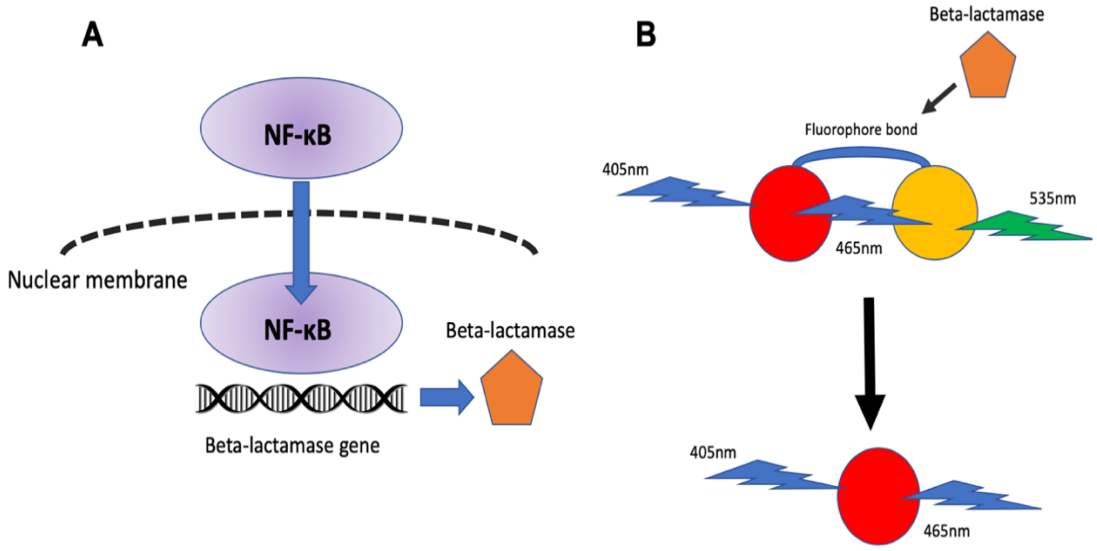

Figure 1. Diagram of the NF-kB FRET assay by the THP-1 CellSensor NF-κB-bla reporter cell line. The NF-kB FRET assay was used to determine the levels of activation of NF-kB in the CellSensor® NF-κB-bla THP-1 cell line where THP-1 cells had been modified with insertion of the NF-κB-bla construct through lentivirus. (A) These cells contain a beta-lactamase reporter gene regulated by the NF-κB complex which promotes the production of beta-lactamase following its activation. (B) The FRET assay measures the emission wavelengths following excitation with a 405 nm (blue) wavelength. Without the presence of beta-lactamase, two fluorophores are linked by a fluorophore bond. Following the initial 405 nm excitation wavelength of the first fluorophore, an emission wavelength of 465 nm (blue) is emitted which in turn serves as the excitation for the adjacent fluorophore. Excitation of the second fluorophore with a 465 nm wavelength consequently leads to an emission wavelength of 535 nm (green). However, activation of the NF-κB complex causes cleavage of the fluorophore bond by the synthesized beta-lactamase, thereby preventing transmission of the 465 nm wavelength to the secondary fluorophore. Higher levels of blue emission signal compared to green emission signal in the measured blue/green ratio indicate higher levels of NF-κB activation.

2 Methods

2.1 Mice

Wild type C57BL/6 mice were purchased from The Jackson Laboratory (Bar Harbor, Maine, USA) and acclimated for a minimum of 48 hrs prior to use. Other mice were acquired as breeder pairs and were maintained and bred in a University of California San Diego Animal Facility accredited by the American Association for Accreditation of Laboratory Animal Care. Animal experiments were carried out according to protocols approved by the Institutional Animal Care and Use Committee of the University of California San Diego. Mice were housed up to four per standard cage at room temperature while on a 12 hr light-dark cycle with all testing conducted during the light cycle. Food and water provided *ad libitum*.

KRN T cell receptor (TCR) mice were a gift from Drs. D Mathis and C. Benoist (Harvard Medical School, Boston, Massachusetts, USA) and the Institut de Génénetique et de Biologie Moléculaire et Cellulaire (Strasbourg, France). Mice were maintained on a C57BL/6 background (K/B). Crossing of K/B mice with NOD/Lt (N) mice produced arthritic mice (K/BxN). NOD/Lt acquired from The Jackson Laboratory (Bar Harbor, Maine, USA).

2.2 Passive serum transfer of arthritis

Blood from arthritic adult K/BxN mice 6-8 weeks old was collected and sera was pooled through spinning of blood down at 14000 rpm for 10 min in a Beckmann table top centrifuge. Pooled sera containing GPI autoantibodies was administered to recipient mice by intraperitoneal (IP) injection (100µL on day 0

and day 2). To assess inflammation in mice, ankle width was measured with a caliper. On the day of sacrifice, mice were bled and hind paws were removed and fixed in 10% formaldehyde.

2.3 Von Frey behavioral testing

The up-down method was used to evaluate mechanical withdrawal thresholds (Chaplan et al., 1994). Mice were placed in clear, plastic cages with wire mesh bottoms 45 min prior to initiation of testing. Von Frey hairs ranging from 2.44 to 4.31 (0.03 g to 2.00 g) were used to measure tactile threshold (Seemes Weinstein von Frey anesthesiometer; Stoelting Co., Wood Dale, IL, USA). Prior to day 0 of the experiment, mice were acclimated by placing in respective cages for 45 minutes for two consecutive days (day -2 and day -1). On the day immediately prior to day 0, mice were exposed on ten times on each paw with the 4.17 filament. The force of the von Frey hair to which the mouse reacts to 50% of the presentations (50% probability withdrawal) was recorded. Mechanical values for both paws were evaluated and averaged for a single data point per day of measurement.

2.4 RNA extraction and quantitative real-time PCR (qPCR)

RNA from flash frozen spinal cords was extracted with a QIAzol Lysis Reagent and the RNeasy Lipid Mini Kit (QIAGEN) in accordance with the manufacturer's protocol. qScript cDNA SuperMix (Quanta Biosciences) was used to prepare complimentary DNA. TaqMan Universal PCR mastermix and predesigned primer and probe sets was used to perform qPCR (Applied

Biosystems, Carlsbad, CA, USA) using a Bio-Rad iCycler with the MyiQ Optical Module (Bio-Rad, #576BR). Three housekeeping amplicons: 18S, Ywhaz (Mm03950126_s1), and β-actin (Mm02619589_g1: Applied Biosystems) were used to calculate a geometric mean and normalize reactions measured in duplicate. Gene specific primers included: Tnf (Mn00443258_m1), Ifnb (Mm00439552_s1), Il10 (Mm00439614_m1), (purchased from Applied Biosystems).

2.5 Compound Library

A compound library of 166,304 chemical entities from eight suppliers was acquired from the UCSF Small Molecule Discovery Center.

2.6 High Throughput Screening and Statistical Analysis

HTS of the chemical library was conducted by Thermo Fisher Scientific at their commercial facility (Madison, WI) in 384-well plates using Cellsensor THP-1 cells. The screen was conducted with LPS alone (LPS 12 hr) as a positive control and 0.5% DMSO as a negative control. A screen was also conducted on cells treated with compounds at 5 hrs without LPS stimulation. This 5 hr screen also which included an LPS alone treatment to use as a positive control. Following background subtraction of the average of the cell-free wells, emission ratios were calculated as the fluorescence density ratio values at two wavelengths. Data was normalized for both timepoints to the 5 hr LPS control.

2.7 Cells and Reagents

The CellSensor NFκB-bla human monocytic THP-1 cell line was purchased from Thermo Fisher Scientific (Waltham, MA). The cell line contains a beta-lactamase reporter gene stably integrated under the regulation of NF-κB. Activation of the NF-κB protein complex results in the production of beta-lactamase, which causes a shift in the fluorescence emission of the beta-lactamase substrate (Live BLAzerTM-FRET B/G (CCF4-AM), Thermofisher) to favor coumarin (460 nm emission) over fluorescein (530 nm emission).

THP-1 cells were purchased from the American Type Culture Collection (Manassas, VA). The RAW264.7 cell line (mouse leukemic monocyte macrophage) was obtained from the American Type Culture Collection. RAW cells were cultured in DMEM (Irvine Scientific, Irvine, CA) supplemented with 2 mM L-glutamine, 100 U/mL penicillin/100 µg/mL streptomycin, and 10% heat-inactivated fetal bovine serum. Mouse primary bone marrow-derived dendritic cells (BMDCs) were isolated from bone marrow of C57BL/6 mice femurs (Datta et al. 2003). LPS *E.coli 0111:B4* (Sigma-Aldrich) was used for the HTS, and LPS-EB Ultrapure (cat# tlrl-3pelps, Invivogen) was used for subsequent assays.

2.8 Measurement of NF-κB Activation by CellSensor NF-κB-bla THP-1 Cells

96-well plates were plated with 5 x 10^4 CellSensor NF-κB-bla THP-1 cells per well in RPMI. RPMI was supplemented with 10% dialyzed fetal bovine serum (Omega Scientific, Inc., Tarzana, CA), 0.1 mM nonessential amino acids, 100 U/mL penicillin, 100 µg/mL streptomycin, and 1 mM sodium pyruvate

(Thermo Fisher Scientific). LPS-EB was added at 10 ng/mL to the wells. Cells treated at respective incubation times in an environment with 5% CO_2 at 37˚C.

Following incubation, LiveBLAzer FRET B/G Substrate (CCF4-AM) was added to the samples (prepared according to the manufacturer's instructions). Samples with substrate were incubated for 2 hrs in the dark at room temperature. A Tecan Infinite M200 plate reader (Männedorf, Switzerland) was used to measure fluorescence at an excitation wavelength of 405 nm and emission wavelengths of 465 and 535 nm. Emission ratios were calculated as the ratio of background-subtracted fluorescence intensities at 465 nm to background-subtracted fluorescence intensities at 535 nm. Background values were taken from cell free wells at the same fluorescence wavelength and subtracted from the raw fluorescence intensity values (Chan et al. 2017).

2.9 Compound Treatment of Cells and Cytokine Evaluation through ELISA

THP-1 cells, RAW cells, and murine BMDCs were plated at 10^5 cells/mL, 10^4cells/mL, and 10^5 cells/mL, respectively in 96-well plates. Cells were then treated with compounds at various concentrations or vehicle in the presence of an agonist overnight. Supernatant was harvested and secreted levels of IL-8, TNFα, IL-6, IFNβ, IL-10, and IP10 were assessed by ELISA according to the manufacturer's protocol (R&D Systems).

2.10 Cell Viability Assays

Following incubation of cells with respective treatment in 96-well plates, supernatant media extracted. A solution of MTT in assay media (0.5 mg/mL)

was added to each well and incubated overnight at 37˚C. MTT (3-[4,5-dimethylthiazol-2-yl]-2,5-dipheyl tetrazolium bromide) was purchased from Acros Organics. Cell lysis buffer (15% w/v SDS and 0.12% v/v 12 N HCl aqueous solution) was then added and incubated overnight. Absorbance of the samples was then measured with a plate reader at 570 nm using 650 nm as a reference.

2.11 Administration of Repurchased Inhibitor compounds in a K/BxN Mouse Model

200mM stock of R-INH compounds was prepared in DMSO. 750 nmol suspension of compound was made in 300 µL of PBS. Compound was administered twice daily via IP injection. Vehicle treated mouse was treated with a 1.25% DMSO solution in PBS.

3. Results

3.1 Role of TLR4 in Allodynia and Cytokine Expression

In previous experiments to investigate differences between WT and TLR4$^{-/-}$ mice, both sexes from the two groups of mice were injected with K/BxN arthritis serum. Analysis of their ankle swelling and pain development over 28 days revealed that there were no significant differences in the development and resolution of ankle swelling across genders and strains (Woller et al. 2018). However, assessment of allodynia through von Frey testing revealed differences in how the four groups of mice developed and recovered from pain. Comparison of WT males and females showed that females recovered from pain while males experienced persistent pain despite resolution of swelling. However, *Tlr4*$^{-/-}$ males showed resolution of pain when compared to WT males. *Tlr4*$^{-/-}$ females showed better attenuation of allodynia when compared to both WT females and *Tlr4*$^{-/-}$ males (Woller et al. 2018).

To investigate TLR4-associated cytokines in these mice and their roles in the development of allodynia, spinal cords of these mice were harvested on day 10 following administration of K/BxN serum. Analysis of mRNA transcripts extracted from the spinal cords revealed a significant decrease in *Tnf* expression levels and an increase in *Ifnb1* levels in *Tlr4*$^{-/-}$ males when compared to WT mouse groups (Figure 2A, B). WT female mice had less *Tnf* transcripts when compared to WT males and *Tlr4*$^{-/-}$ mice expressed lower levels of *Tnf* in males and higher levels of *Ifnb1* when in males compared to females. *Tlr4*$^{-/-}$ male mice expressed greater levels of *Il10* transcripts when compared to WT males and *Tlr4*$^{-/-}$ females while *Tlr4*$^{-/-}$ females showed less *Il10* mRNA

expression compared to their WT counterparts (Figure 2C). The results from these investigations show that increased levels of *Ifnb1* and *Il10* mRNA expression levels on day 10 were beneficial and associated with at least partial recovery from chronic allodynia. In contrast, groups with high spinal levels of TNFα were more likely to develop persistent allodynia. Hence an agent that would decrease TNFα and increase IFNβ or IL-10 cytokine levels might be a potential therapeutic to treat chronic arthritis pain.

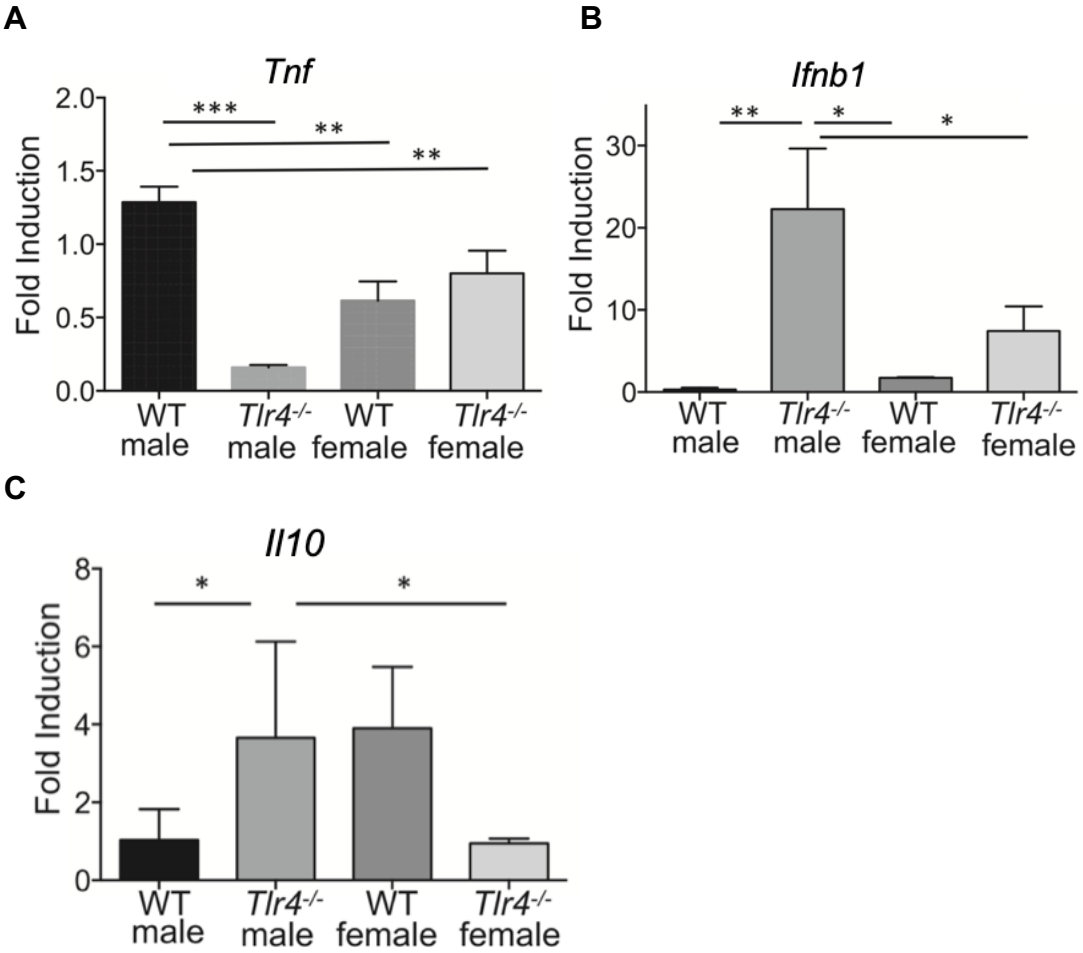

Figure 2. TLR4 deficiency manifests differences in cytokine mRNA expression in the spinal cord. Spinal cords were harvested from WT and *Tlr4*$^{-/-}$ mice (4/group) on day 10 after the administration of K/BxN serum. Spinal cord tissues were analyzed for differences in *Tnf* (A), *Ifnb1* (B), and *Il10* (C) expression. WT male mice show significantly elevated *Tnf* mRNA on day 10 relative to *Tlr4*$^{-/-}$ mice, while *Tlr4*$^{-/-}$ mice show significantly elevated levels of Ifnb1 and Il10. Data are represented as mean ± SEM and * indicates $p < 0.05$, **$p < 0.01$, ***$p < 0.001$.

Section 3.1 Role of TLR4 in Allodynia and Cytokine Expression, in part, is a reprint of the material as it appears in Neuraxial TNF and IFN-beta co-modulate persistent allodynia in arthritic mice 2018. Woller, Sarah A.; Ocheltree, Cody; Wong, Stephanie Y.; Bui, Anthony; Fujita, Yuya; Gonçalves dos Santos, Gilson; Yaksh, Tony Y.; Corr, Maripat, Brain, Behvavior, and Immunity, 2018. The thesis author was a co-author of this paper.

3.2 Analysis of Existing HTS Screens

In prior studies, an HTS was conducted on a chemical library of 166,304 compounds through the use of a CellSensor NF-κB-bla reporter in THP-1 cells, a human monocytic cell line. To identify novel small-molecule compounds as potential immunomodulators of TLR pathways, we aimed to discriminate compounds that suppressed innate immune stimulation by lipopolysaccharide (LPS), a TLR4 ligand. Each of the 166,304 compounds in the chemical library was tested on the CellSensor NF-κB-bla reporter for intrinsic NF-κB activity at 5 hrs without LPS stimulation and NF-κB activity after 12 hrs of incubation with LPS as a primary stimulant (Chan et al. 2017). Data from both HTS were normalized to the LPS-induced NF-κB activity levels following a 5 hr incubation (Figure 3).

Compounds with known biological properties were also included in the library and their readouts from the FRET assay were organized into clustered data regions (Figure 3). The three main compound clusters were glucocorticoids, COX inhibitors, and gonadal steroids (Table 2). To segregate compounds with the greatest potential as immunosuppressants, compounds which had similar activity as the glucocorticoid cluster region were chosen for further screening. To avoid compounds that have an intrinsic activation or inhibition of NF-κB, compounds that had -10 to 0% activation levels of NF-κB at 5 hrs were selected. To further identify compounds that suppress NF-κB activity compared to existing gonadal steroids, compounds were further screened for having 30% or less NF-κB activity at a 12 hrs incubation with LPS stimulation. A total of 1843 compounds were selected from the glucocorticoid

region of the HTS data that fit the activation thresholds set at each respective timepoint.

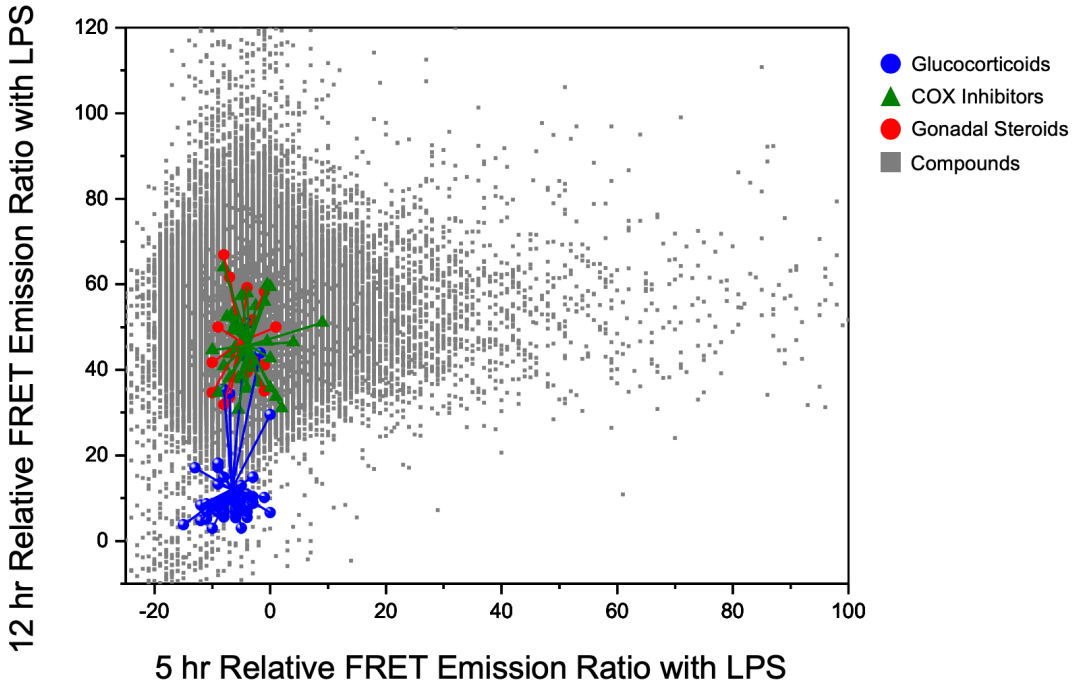

Figure 3. Segregation of potential immunosuppressants from other related bioactives through HTS analysis of NF-κB activation. HTS were conducted to identify compounds that would suppress NF-κB activation by a stimulus from lipopolysaccharide (LPS), a TLR4 ligand. The data from two prior HTS were analyzed by clustering data from known compounds from gonadal steroid, COX inhibitor, and glucocorticoid groups included in the screened chemical library. Compounds near the glucocorticoid cluster region were picked for further assessment of immunosuppressant activity.

Table 2. Known compounds included in HTS Library.

Cluster Groups	Compounds
COX Inhibitors	Acetaminophen Diclofenac Flufenamic Acid Ibuprofen Ketoprofen Ketorolac Piroxicam Rofecoxib Salicylic Acid Sulindac
Glucocorticoids	Budenoside Clobetasol Cortisone Dexamethasone Fluoroetholone Halcinonide Hydrocortisone Mometasone Prednisolone Triamcinolone
Gonadal Steroids	Ethisterone Formestane Hydroxyprogesterone Methyltestosterone Norethindrone Norgestrel Oxymetholone Pregnenolone Progesterone Testosterone

3.3 Confirmation Screen and Kinetic Profiling

Using the new analysis of the prior two HTS screens, 1,843 compounds that expressed similar FRET reporter activity to known glucocorticoids included in the original chemical library were selected for a secondary confirmation of suppression of LPS-induced NF-κB activity. These selected hits from the main HTS screens were evaluated in duplicate in a confirmation screen using the same THP-1 CellSensor NF-κB-bla reporter assay. The effect of these compounds on NF-κB activity was evaluated following incubation of these compounds with THP-1 cells and LPS stimulation at 5 hr and 16 hr to assess their kinetic suppression profiling (Figure 4). Analysis of the compound behavior at the 5 hr timepoint against the 16 hr timepoint shows a greater number of compounds with lower NF-κB activity following a longer incubation time versus the shorter time (Figure 4B). These confirmation screens included dexamethasone (DEX), one of the known glucocorticoids in the HTS, and 5-(4-fluorophenyl)-2-ureido-thiophene-3 carboxylic acid amide (UTC), a known IKK-β inhibitor that suppresses NF-κB activity (Podolin et al. 2005; Endo et al. 2012).

To select compounds with potential as possible immunosuppressants, hit compounds were discriminated through an enrichment strategy based on a naïve standard activity-based approach (naïve “Top X” approach) and chemoinformatic clustering. For the Top X approach, desired activity threshold levels of NF-κB activity were arbitrarily designated at ≤ 50% and ≤ 25% of the normalized FRET emission ratios at 5 hr and 16 hr, respectively. Compounds which passed both of these requirements were selected for further assessment (Figure 5).

In addition to the compounds chosen through the Top X approach, compounds of similar chemotype clusters as the Top X-selected compounds were added to the selection group as potential candidates as immunomodulators. Compounds which had ≤ 84% and ≤ 68% relative emission ratio at 5hr and 16hr, respectively, with compound cluster sizes ≥ 3 and chemotypes similar to the Top X compounds were selected. Compounds which had ≥ 68% and ≤ 25% relative emission ratio at 5 hr and 16 hr, respectively, with compound cluster sizes ≥ 2 with chemotypes unrelated to the Top X selected compounds were also selected. Using both the Top X approach and chemotype selection, a total of 270 compounds were identified from this screening. These compounds were designated to be further assessed for their effects on cell viability and suppression of NF-κB-associated cytokine production.

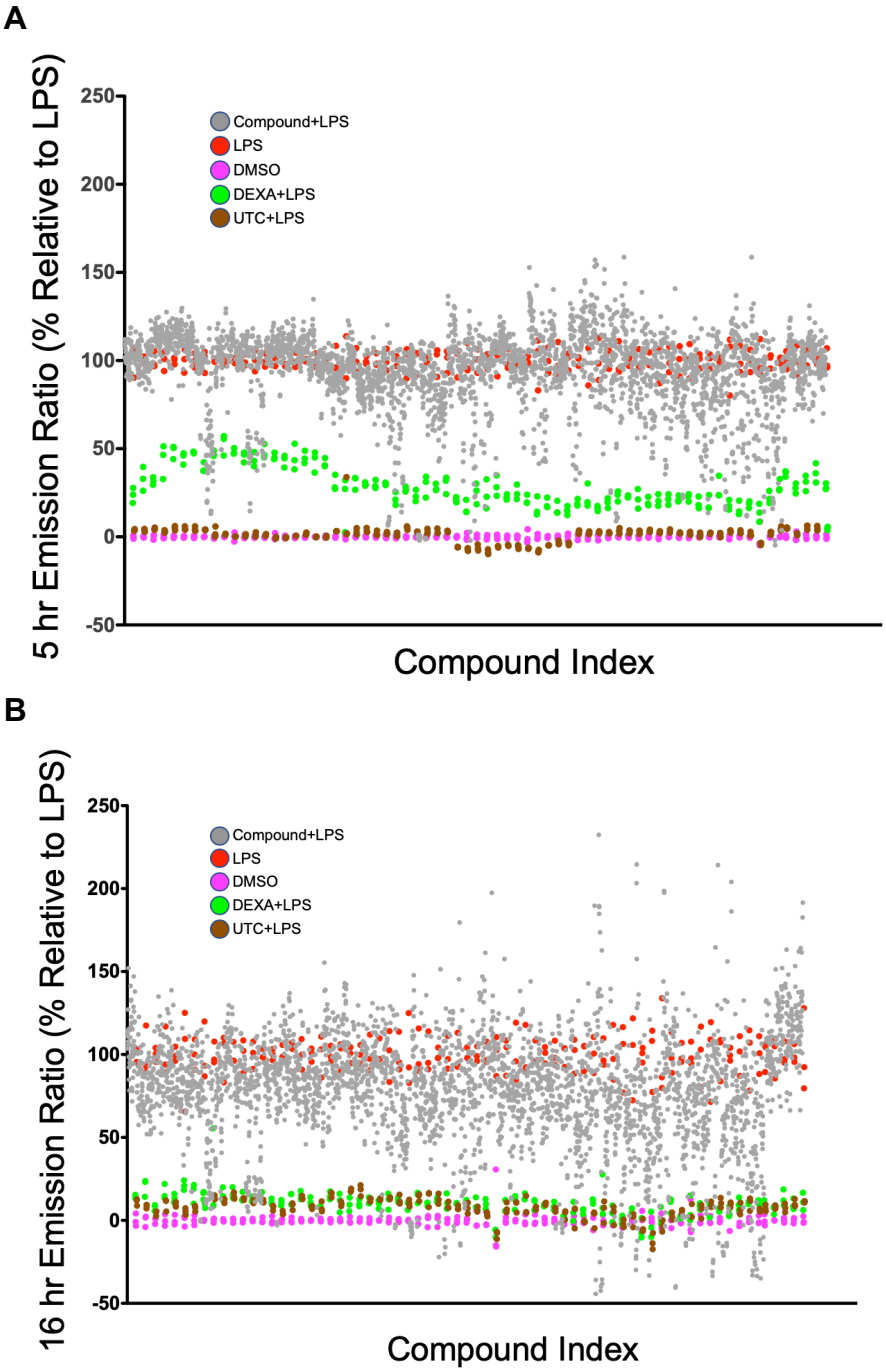

Figure 4. Suppression of LPS-induced NF-κB activity in THP-1 cells by 1843 selected compounds at 5 hr and 16 hr. (A) Compound data from the 5 hr FRET assay are shown. (B) Compound data from the 16 hr FRET assay are shown.

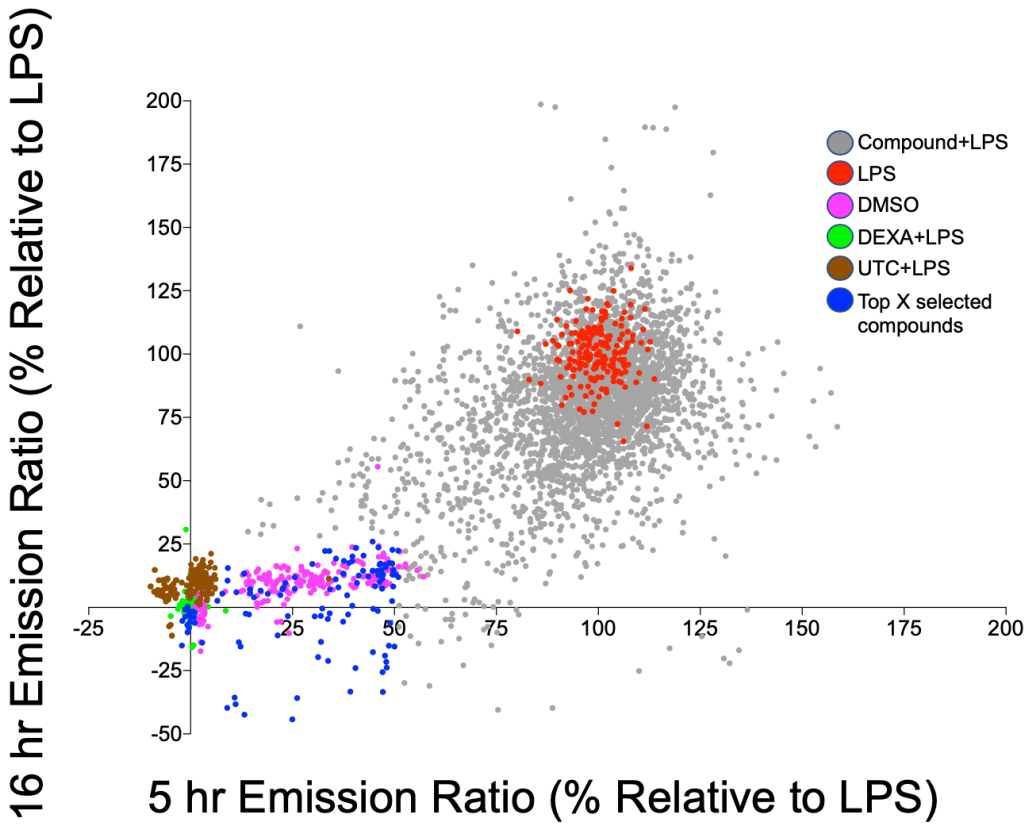

Figure 5. Top X selection of 270 compounds after co-incubation with LPS for 5 hours and 16 hours in THP-1 cells. Candidate compounds were analyzed by a CellSensor NF-κB-bla reporter FRET assay in THP-1 cells at 5 h and 16 h timepoints. THP-1 CellSensor cells were plated 10^5 cells/well in 96-well flat plates bottom with 16 compounds in duplicates per plate. Cells were treated with compounds at 5μM concentrations following stimulation by 10ng/mL LPS. All assay runs included DMSO (pink), DMSO+LPS (red), DEXA+LPS (green), and UTC+LPS (brown) controls. Gray dots represent the duplicate data of each of the tested compound candidates. A) Data from both timepoints are shown and blue dots represent compounds expressing 0.5 or less reporter activity relative to the DMSO+LPS control at 5 h and 0.25 or less activity at 16 h. 270 compounds were selected from this assay for subsequent screening.

3.4 Evaluation of Cytotoxicity and Cytokine Production in THP-1 Cells

Following selection of compounds using the naïve Top-X approach and chemoinformatic clustering, the 270 candidate drugs were evaluated for their effects on cell viability and ability to suppress NF-κB-associated cytokines (Figure 6). THP-1 cells were incubated overnight following treatment with LPS stimulation and 5μM of the 270 selected compounds. Following incubation, the media supernatant was removed and the production of human IL-8 (hIL-8), an NF-κB-associated interleukin (IL), of cells treated with each respective compound was assessed via ELISA (Figure 7). Figure 7A shows the relative hIL-8 production normalized to the LPS control in order of increasing levels of cytokine production. Compounds which showed suppressed activation of IL-8 at 70% or lower relative to DMSO treatment were identified as potential candidates for future evaluation as immunosuppressants.

To assess the cytotoxicity effects of the compounds, MTT (3-(4,5-dimethylthiazol-2-yl)-2,5-diphenyltetrazolium bromide) assays that assess metabolic activity of cells were conducted on the treated THP-1 cells following removal of the supernatant media. Assessment of the colorimetric changes after MTT treatment indicated the relative viability of compound-treated cells compared to control cells treated with LPS (Figure 7B). Compounds which showed a viability of 90% or higher relative to the control were identified as potential candidates for future testing. Comparison of the relative hIL-8 production of treated cells with their respective viability reveals a positive correlation between hIL-8 levels and cytotoxicity. Compounds which met both of the set requirements of effecting a suppression of hIL-8 while maintaining a

high cellular viability in the cytokine and cytotoxicity assays were identified as potential immunomodulators for subsequent testing.

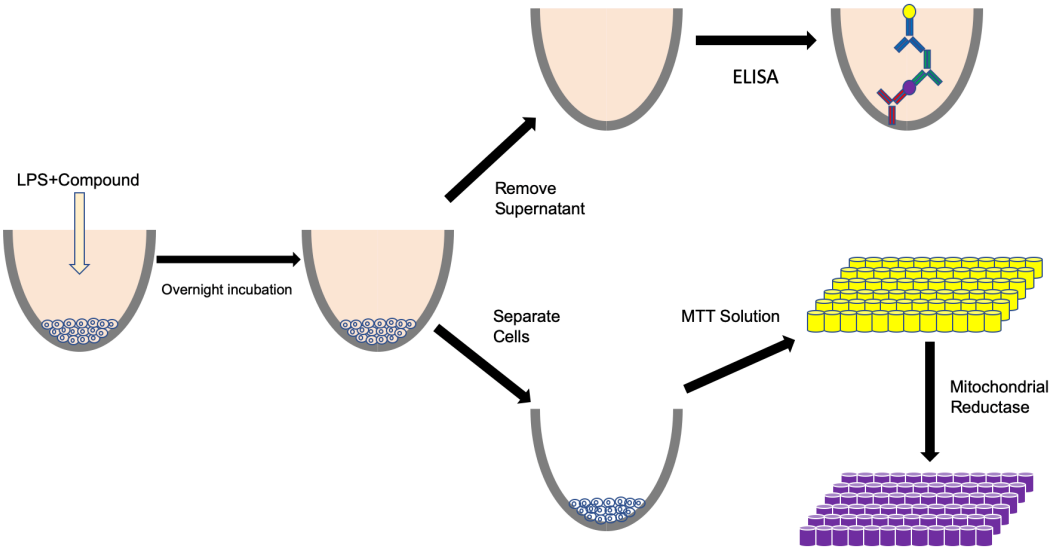

Figure 6. Cytokine and cytotoxicity evaluation assay diagram. Cells stimulated with an agonist are treated with compound and incubated overnight. Following incubation, supernatant is removed from cells to be analyzed via ELISA. Cells are treated with an MTT solution overnight before addition of a mitochondrial reductase solution. Following overnight incubation with mitochondrial reductase, samples are evaluated to determine relative cytotoxicity of each respective treatment.

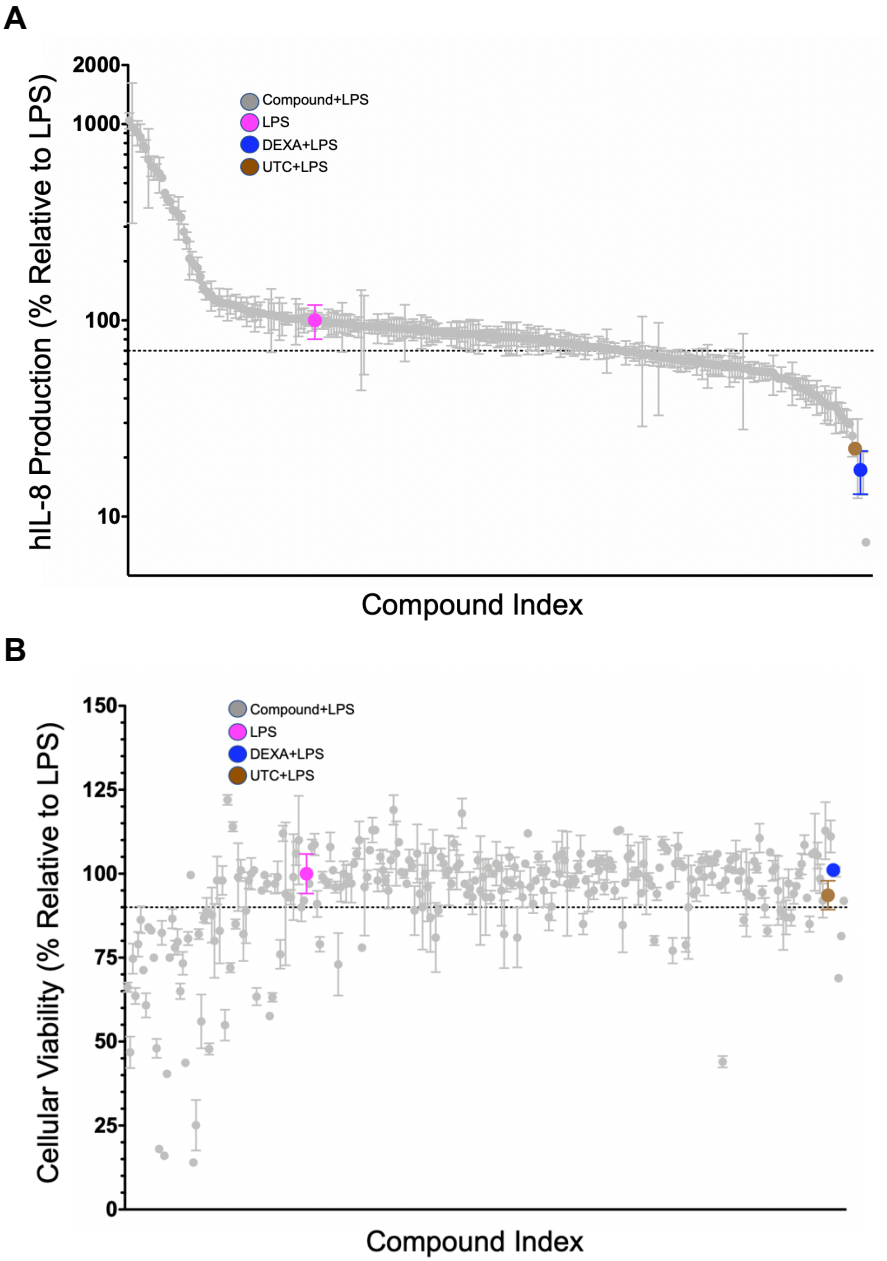

Figure 7. Relative hIL-8 production and cellular viability of THP-1 cells treated with 270 selected compounds. 270 compounds selected following confirmation screening of were analyzed for cytokine production and cellular viability. (A) Supernatants extracted following incubation of THP-1 cells for 16 hours with dual treatment of 10 ng/mL LPS stimulation and 5μM of compound was analyzed via hIL-8 ELISA. Results were normalized relative to the LPS control. The dotted line indicates 70% production of hIL-8 relative to the DMSO control. (B) The 270 compounds selected from the confirmation NF-kB FRET Assay were then tested for viability through an MTT assay in THP-1 cells. Viability was determined through normalization of results to the LPS control. The dotted line represents 90% viability relative to the LPS control. Data shown as mean ± SD of triplicate data.

3.5 Validation of Repurchased/Resynthesized Compounds

Compounds which met the viability and cytokine thresholds in the confirmation screening were then grouped by their respective chemotypes. A total of 45 compounds in fifteen lead chemotypes and 15 singletons (compounds not associated with a chemotype) were identified which met the appropriate requirements (Table 3). Three of the fifteen chemotypes were excluded from further assessment as their chemical structures identified them as Michael acceptors. Other chemotypes were also excluded based on whether they could be repurchased or resynthesized. From the remaining chemical families, twelve compounds were chosen for validation and further assessment as immunomodulators.

The twelve chosen compounds were then repurchased or resynthesized in larger quantities and named R-INH#1-12. These repurchased compounds were reassessed for their suppression of hIL-8 production in THP-1 cells (Figure 8). THP-1 cells were treated overnight for 16 hrs with the repurchased compounds together with LPS stimulation and levels of hIL-8 produced following each respective treatment were assessed through ELISA. Assessment of the data revealed that half of the twelve inhibitors (R-INH#1-6) reduced the level of hIL-8 levels to 70% or less than that of the LPS control. The other half of the R-INH# compounds did not meet the set criteria and was inconsistent with the data previously seen in their counterparts in the original compound library. Analysis of these compounds from the original library and the R-INH# series showed that several of the compounds in the library had become degraded from their original structures.

Table 3. Number of compounds in lead chemotypes by screening stage. Number of compounds are shown by how many were present in following the confirmation screening and following the cytokine and cytotoxicity assays. Specific exclusion criteria for several chemotypes are also listed.

Chemotype	1843 Compound Screening	Passed Cytokine & Cytotoxicity Assays	Exclusion Criteria
1H-pyrazolo[3,4-d] pyrimidin-4-amine	22	13	Selected
E)-5-benzylideneimidazolidine-2,4-dione	17	4	Exclude because it is a Michael acceptor
Bis-aryl Urea	12	2	Selected
2-Nitro Furan Arylamide	9	5	Selected
Piperidine derivatives	9	3	Weak Inhibition
Quin Molecules	8	3	Exclude because it is a Michael acceptor
1H-pyrazolo[3,4-b]quinolin-3-amine	6	2	No commercial availability
Aryl Substituted Aryl Sulfonamide and Aryl Amide	6	1	No commercial availability
2-imino-1,2-dihydro-5H-dipyrido[1,2-a:2',3'-d]pyrimidin-5-one	5	3	Selected
Piperazine Derivatives	5	1	No commercial availability
Quin-like Pyridine Analogs	3	2	Exclude because it is a Michael acceptor
Thiophene Pyrazine Piperidine	3	2	Selected
Truncated Pyrazole Derivative	22	2	No commercial availability
Pyrazolopyyroolidinone	2	1	Selected
Sulfonamide	2	1	No
Singletons	n/a	15	-

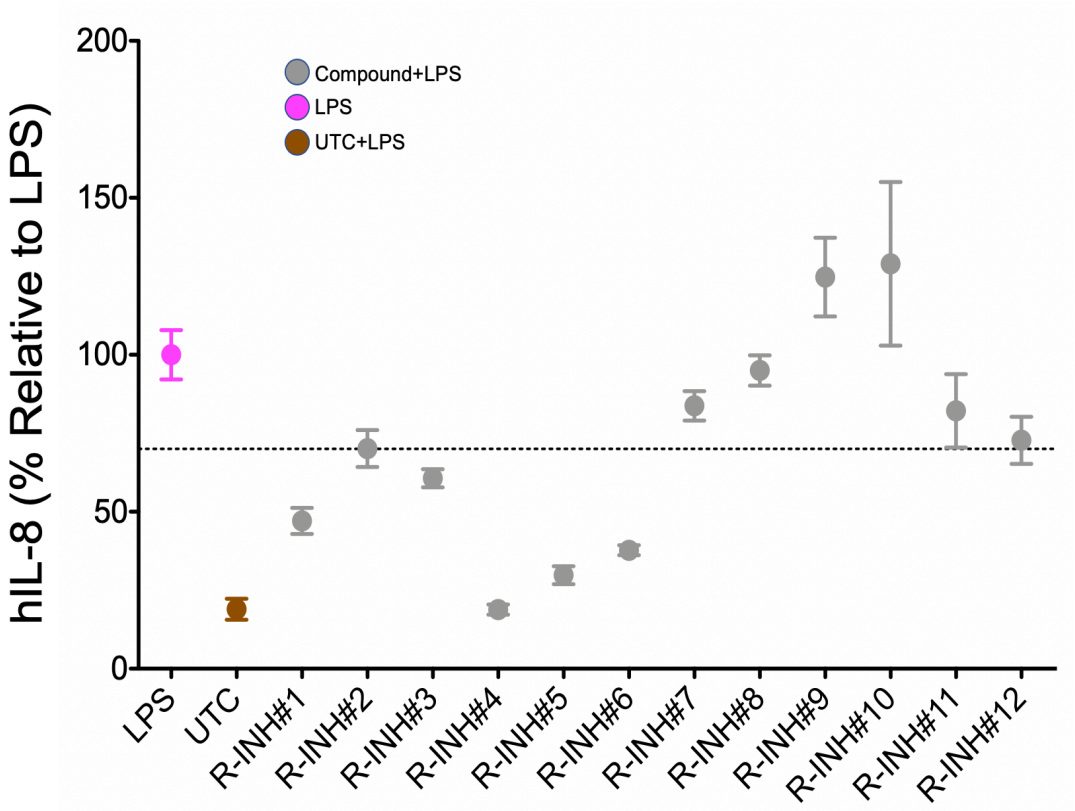

Figure 8. Inhibition of LPS induced hIL-8 production by repurchased compounds. Repurchased compounds were reassessed for their inhibition of LPS-induced hIL-8 production by THP-1 cells after a 16 hr incubation. Levels of hIL-8 production were compared with the DMSO+LPS control. Compounds which expressed 70% or less hIL-8 production activity relative to the control (Compounds R-INH#1-6) were selected for future screening. The mean ± SD are shown.

3.6 Analysis of Repurchased Compounds in Murine Studies

Following evaluation of the compounds in THP-1 cells, the candidate compounds were then investigated for to see whether they retained similar activity in murine cell. To assess the viability and cytokine suppression effects of the candidate compounds in murine studies, the R-INH# compounds were analyzed in RAW cells, a macrophage-like Abelson leukemia virus transformed murine cell line. Compounds were incubated overnight at a 5 μM concentration with LPS stimulation in RAW cells and assessed for production of mTNFα and cellular viability relative to the LPS control (Figure 9A, B). In RAW cells, half of the repurchased compounds were able to suppress production of mTNFα when compared to the LPS control following ELISA on the supernatant (Figure 9A). Furthermore, all of the compounds exhibited high levels of viability relative to the LPS control when compound-treated cells were analyzed through an MTT assay (Figure 9B). Results from these murine in-vitro assays and the previous hIL-8 production analysis of compound treatment THP-1 cells were studied together to select candidates with the highest potential as immunosuppressants (Table 4). Of the twelve compounds chosen for the validation set, R-INH#4-6 from the 2-Nitro Furan Arylamide chemotype passed the screening requirements set for both cell line assays. These compounds were identified as potential immunomodulators that can suppress various cytokines of the innate immune system in both human and mouse models.

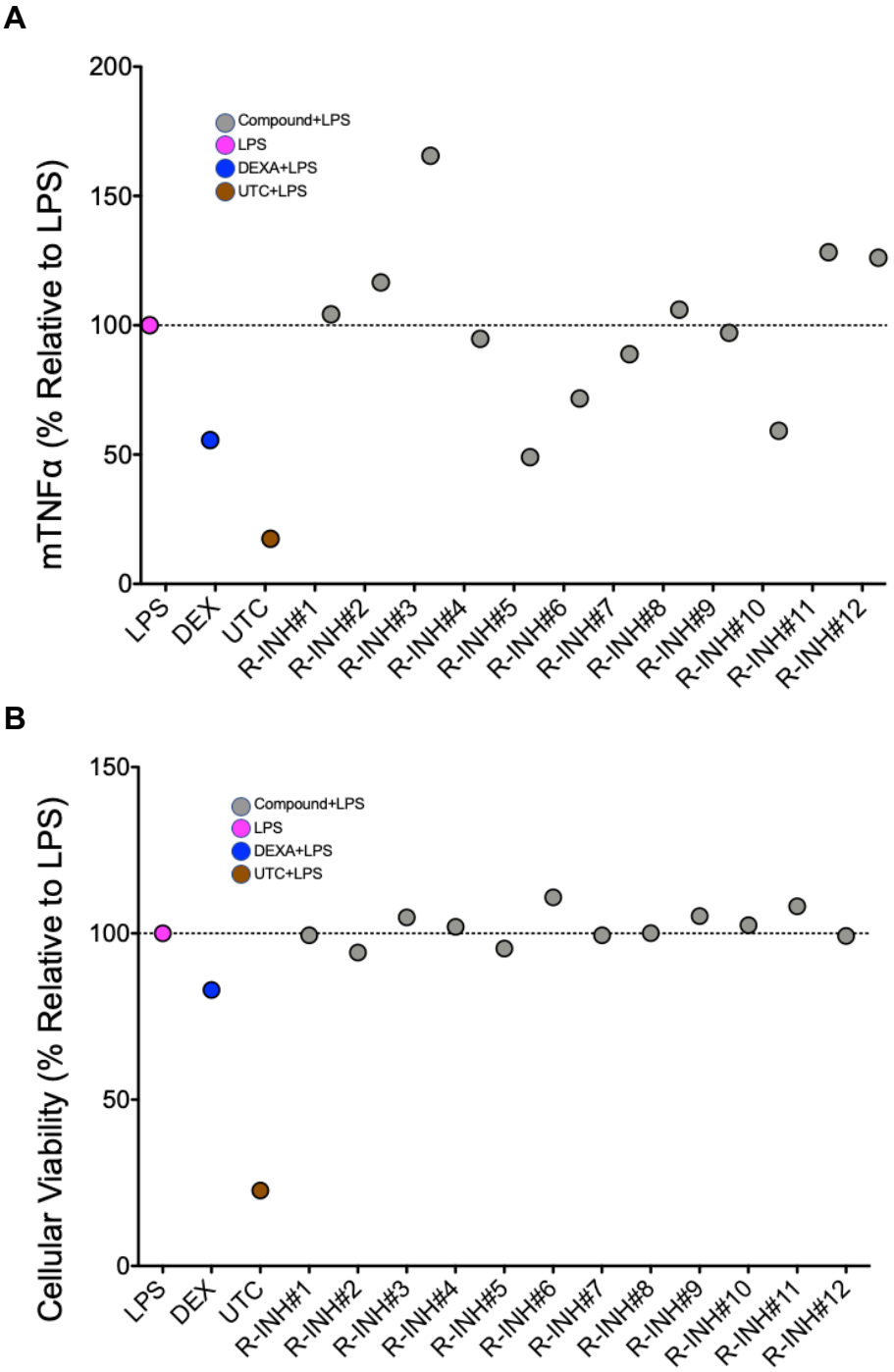

Figure 9. Relative mTNFα production and cellular viability of RAW cells treated with repurchased compounds and LPS. Repurchased compounds were analyzed for cytokine suppression and cellular viability. (A) Supernatant extracted following incubation of RAW cells for 18 hours with dual treatment of 10 ng/mL LPS stimulation and 5μM of compound was analyzed via TNFα ELISA. Results were normalized relative to the LPS control. (B) Repurchased compounds were then tested for viability through an MTT assay in RAW cells. Viability was determined through normalization of results to the LPS control.

Table 4. Summary of validation results of re-purchased compounds.
Repurchased compounds which failed to meet the set cytokine levels are in red.

Compound	Chemotype	MW (g/mol)	% Cellular Viability	Relative hIL-8 Production (Screening)	Relative hIL-8 Production THP-1 Cells (Repurchased)	Relative mTNFα Production Raw Cells (Repurchased)
R-INH#1	1H-pyrazolo[3,4-d] pyrimidin-4-amine	321.43	98.70	50.60%	47.10%	104.22%
R-INH#2	1H-pyrazolo[3,4-d] pyrimidin-4-amine	295.39	100.10	62.70%	70.10%	116.55%
R-INH#3	bis-aryl urea	261	105.60	50.60%	60.70%	165.54%
R-INH#4	2-Nitro Furan Arylamide	276	98.70	21.90%	18.80%	94.79%
R-INH#5	2-Nitro Furan Arylamide	300	101.80	54.30%	29.80%	48.99%
R-INH#6	2-Nitro Furan Arylamide	312	100.10	66.70%	37.70%	71.66%
R-INH#7	Aryl Substituted Aryl Sulfonamide	409	95.40	65.20%	83.70%	88.86%
R-INH#8	2-imino-1,2-dihydro-5H-dipyrido [1,2-a:2',3'-d]pyrimidin-5-one	453.5	106.10	25.80%	95%	106.05%
R-INH#9	2-imino-1,2-dihydro-5H-dipyrido [1,2-a:2',3'-d]pyrimidin-5-one	453.5	104	32.30%	124.80%	97.07%
R-INH#10	2-imino-1,2-dihydro-5H-dipyrido [1,2-a:2',3'-d]pyrimidin-5-one	453.5	101.40	54.80%	129%	59.19%
R-INH#11	Thiophene Pyrazine Peperidine	416.91	91.30	30.10%	82.20%	128.26%
R-INH#12	Pyrazolopyyroolidione	419.53	100.30	57.80%	72.80%	126.13%

3.7 Specificity of R-INH#4-6 Compound Activity

We next investigated the specificity of these compounds through evaluation of common innate immune pathways. In determining the specificity of the R-INH#4-6 compounds, we primarily focused on innate immune pathways which are associated with the production of TNFα and Type I IFNs. To determine the specificity of R-INH#4-6 and their effects on the production of IFN and other pathway-related cytokines, WT murine BMDCs (bone marrow-derived dendritic cells) were incubated with Poly I:C (50μg/mL), LPS (100ng/mL), IV270 (1μM), ODN 1826 (1.25μM), and DMXAA (10μg/mL) which are ligands for TLR3, TLR4, TLR7, TLR9, and STING, respectively. These BMDCs were also treated with 5 μM of R-INH#4-6 or a DMSO control simultaneously with TLR ligands (TLR-L).

Following an overnight incubation with the compounds and the ligands, the supernatant media from these cells was collected and analyzed for relative production of mTNFα, mIFNβ, mIP10, mIL-6, and mIL-10 through ELISA. Comparison of cytokine production relative to the DMSO treated control revealed that TNFα expression is greatly suppressed with the use of these compounds when stimulated with TLR7, TLR9, and STING ligands (Figure 10C-D). A slight suppression of mTNFα by the compounds following stimulation with LPS was also observed by treatment with R-INH#4 and R-INH#6 following LPS stimulation, but was not greatly observed by R-INH#5 (Figure 10A). R-INH treatment together with stimulation by the STING ligand expressed the greatest relative suppression of mTNFα. When analyzed for relative production levels of mIFNβ, R-INH#4-6 strongly suppressed mIFNβ when stimulated by TLR3,

TLR4, TLR7, TLR9, and STING ligands (Figure 11B-E). However, the LPS-stimulated BMDCs expressed an upregulation of mIFNβ when treated with R-INH#5 (Figure 11A).

Investigation of the effects of the compounds on mIP10 production produced by the treated cells revealed suppression of mIP10 when stimulated with each of the ligands (Figure 12A-D). The TLR3, TLR7, and TLR9 pathways experienced the greatest degree of relative suppression of mIP10. The LPS stimulated cells produced roughly half of the amount of mIP10 when treated with R-INH#4-6. R-INH#5 was most effective in suppression mIP10 associated with the STING pathway (Figure 12E).

Evaluation of relative mIL-6 levels produced by the treated BMDCs revealed that R-INH#4-6 did not have an effect on mIL-6 produced through the TLR4 pathway (Figure 13A). Treatment with R-INH#4-6 suppressed mIL-6 production by the TLR3, TLR7, TLR9, and STING pathways (Figure 13B-D). The greatest suppression by these compounds was observed when stimulated by the TLR3 and STING ligands. mIL-10, an anti-inflammatory cytokine, was also evaluated and was shown to be strongly suppressed when treated with compounds with TLR4, TLR7, and TLR9 ligands (Figure 14).

Comparison of the relative level of cytokine production was conducted with each respective ligand and compound treatment was done to observe how treatment with R-INH#4-6 affect the two pathways (Table 5).

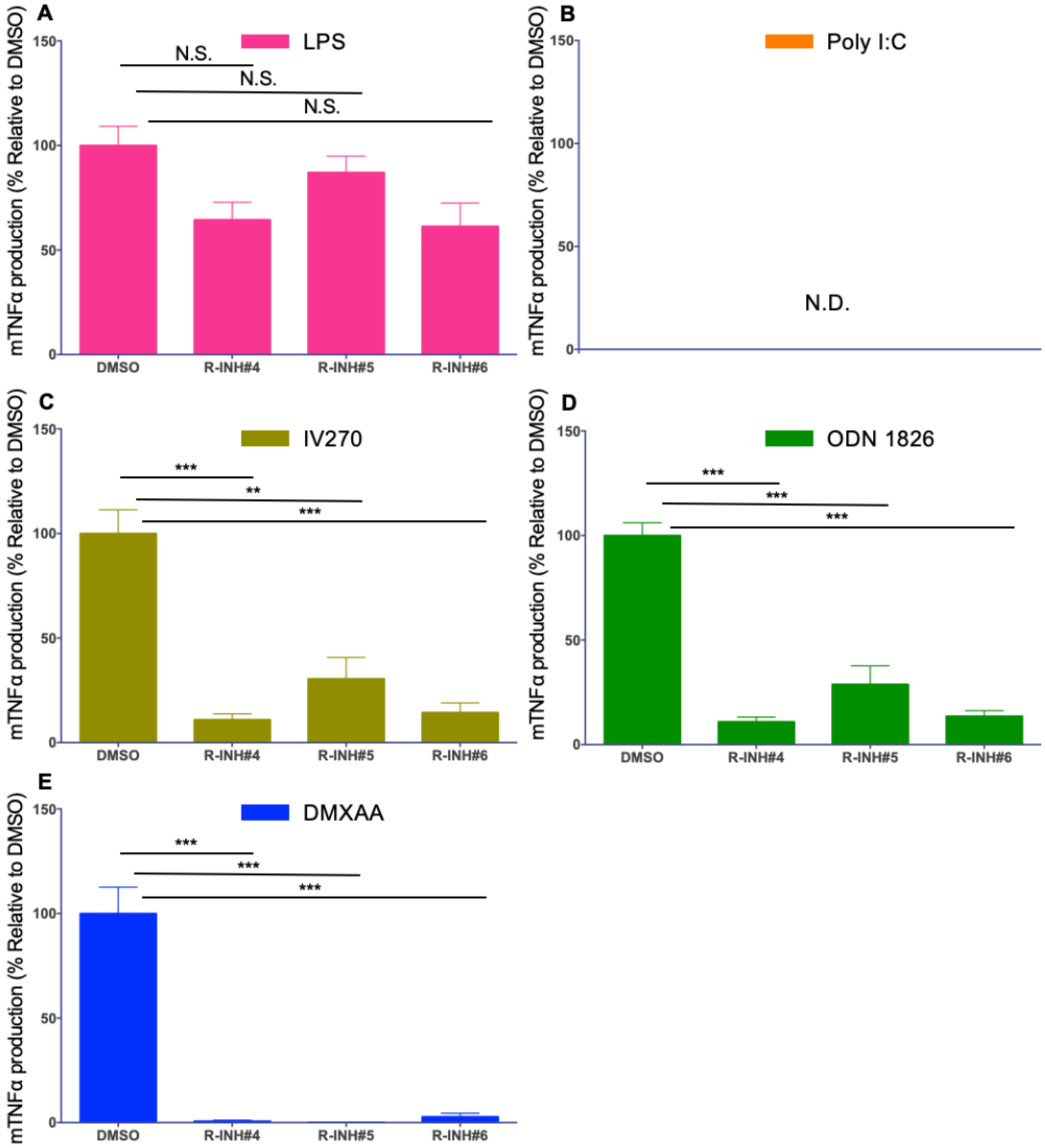

Figure 10. Relative TNFα expression in WT BMDCs following treatment of cells with agonists and R-INH#4-6. (A) mTNFα levels relative to the DMSO control of BMCDs treated with LPS and respective treatments. (B) mTNFα levels relative to the DMSO control of BMCDs treated with Poly I:C and respective treatments. (C) mTNFα levels relative to the DMSO control of BMCDs treated with IV270 and respective treatments. (D) mTNFα levels relative to the DMSO control of BMCDs treated with ODN 1826 and respective treatments. (E) mTNFα levels relative to the DMSO control of BMCDs treated with DMXAA and respective treatments. Data are represented as mean ± SEM and * indicates $p < 0.05$, **$p < 0.01$, ***$p < 0.001$. N.S. – not significant. N.D. – not detected.

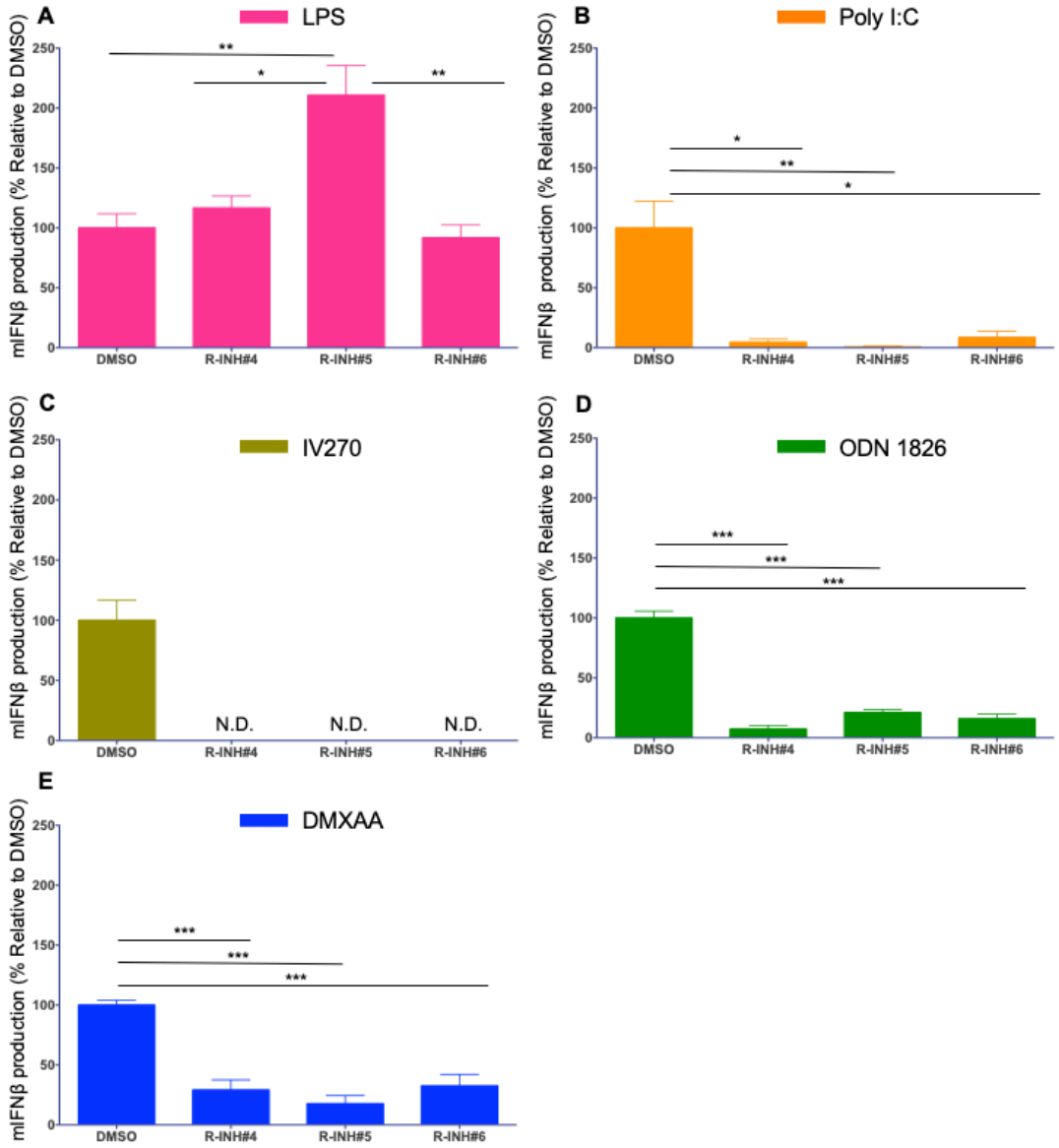

Figure 11. Relative mIFNβ expression in WT BMDCs following treatment of cells with agonists and R-INH#4-6. (A) mIFNβ levels relative to the DMSO control of BMCDs treated with LPS and respective treatments. (B) mIFNβ levels relative to the DMSO control of BMCDs treated with Poly I:C and respective treatments. (C) mIFNβ levels relative to the DMSO control of BMCDs treated with IV270 and respective treatments. (D) mIFNβ levels relative to the DMSO control of BMCDs treated with ODN 1826 and respective treatments. (E) mIFNβ levels relative to the DMSO control of BMCDs treated with DMXAA and respective treatments. Data are represented as mean ± SEM and * indicates $p < 0.05$, ** $p < 0.01$, *** $p < 0.001$. N.S. – not significant. N.D. – not detected.

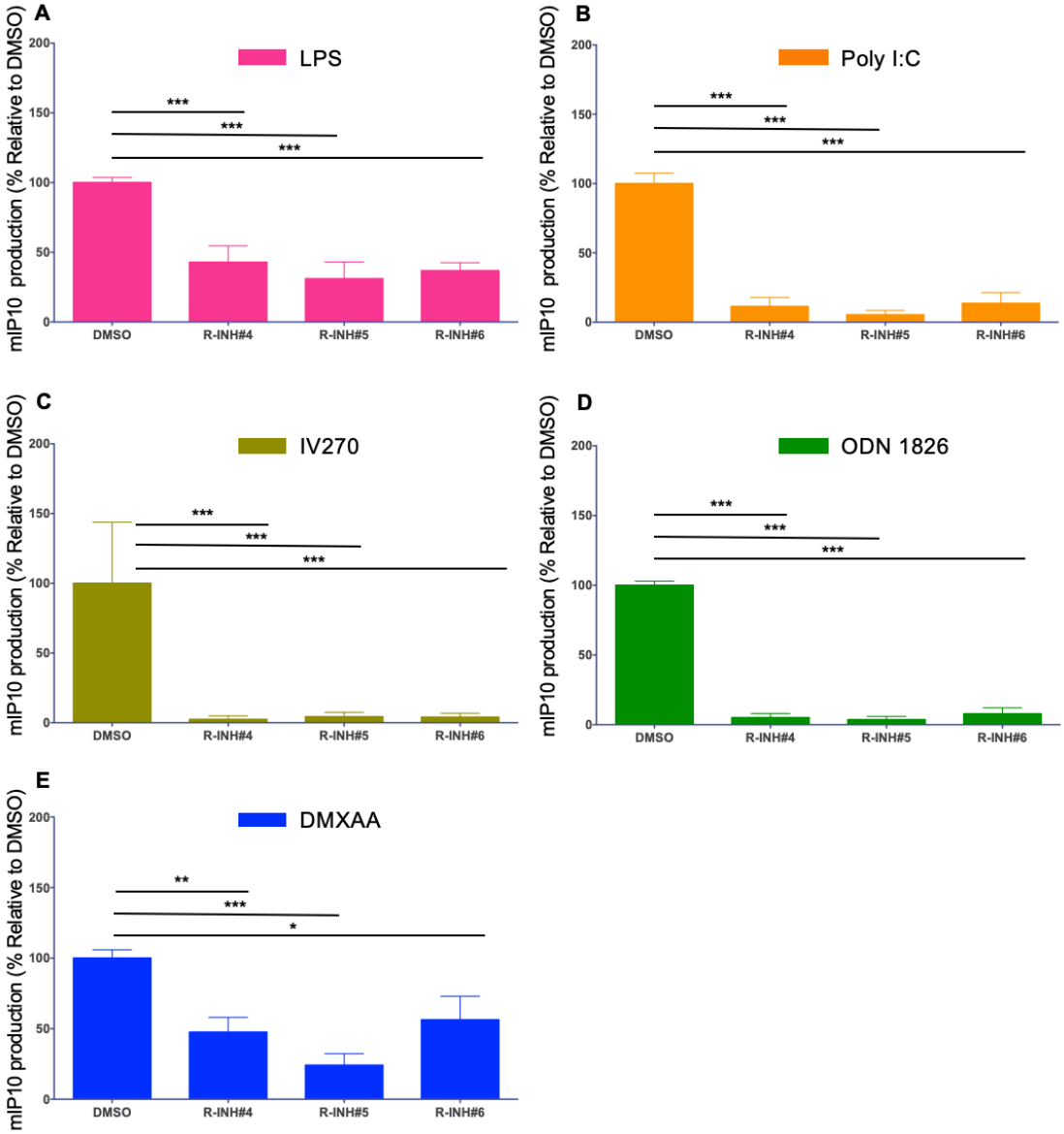

Figure 12. Relative mIP10 expression in WT BMDCs following treatment of cells with agonists and R-INH#4-6. (A) mIP10 levels relative to the DMSO control of BMCDs treated with LPS and respective treatments. (B) mIP10 levels relative to the DMSO control of BMCDs treated with Poly I:C and respective treatments. (C) mIP10 levels relative to the DMSO control of BMCDs treated with IV270 and respective treatments. (D) mIP10 levels relative to the DMSO control of BMCDs treated with ODN 1826 and respective treatments. (E) mIP10 levels relative to the DMSO control of BMCDs treated with DMXAA and respective treatments. Data are represented as mean ± SEM and * indicates $p < 0.05$, **$p < 0.01$, ***$p < 0.001$. N.S. – not significant. N.D. – not detected.

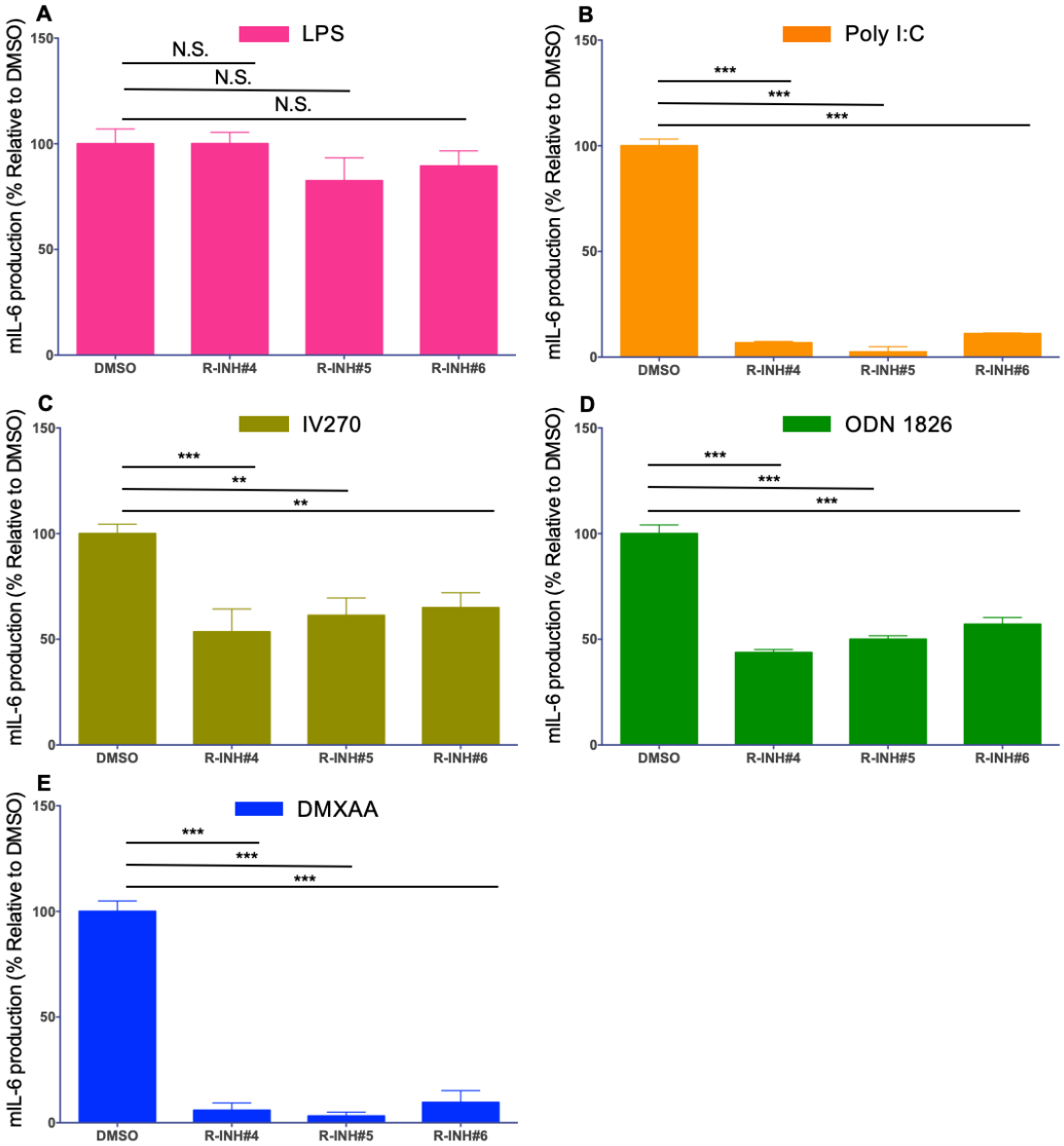

Figure 13. Relative mIL-6 expression in WT BMDCs following treatment of cells with agonists and R-INH#4-6. (A) mIL-6 levels relative to the DMSO control of BMCDs treated with LPS and respective treatments. (B) mIL-6 levels relative to the DMSO control of BMCDs treated with Poly I:C and respective treatments. (C) mIL-6 levels relative to the DMSO control of BMCDs treated with IV270 and respective treatments. (D) mIL-6 levels relative to the DMSO control of BMCDs treated with ODN 1826 and respective treatments. (E) mIL-6 levels relative to the DMSO control of BMCDs treated with DMXAA and respective treatments. Data are represented as mean ± SEM and * indicates $p < 0.05$, **$p < 0.01$, ***$p < 0.001$. N.S. – not significant. N.D. – not detected.

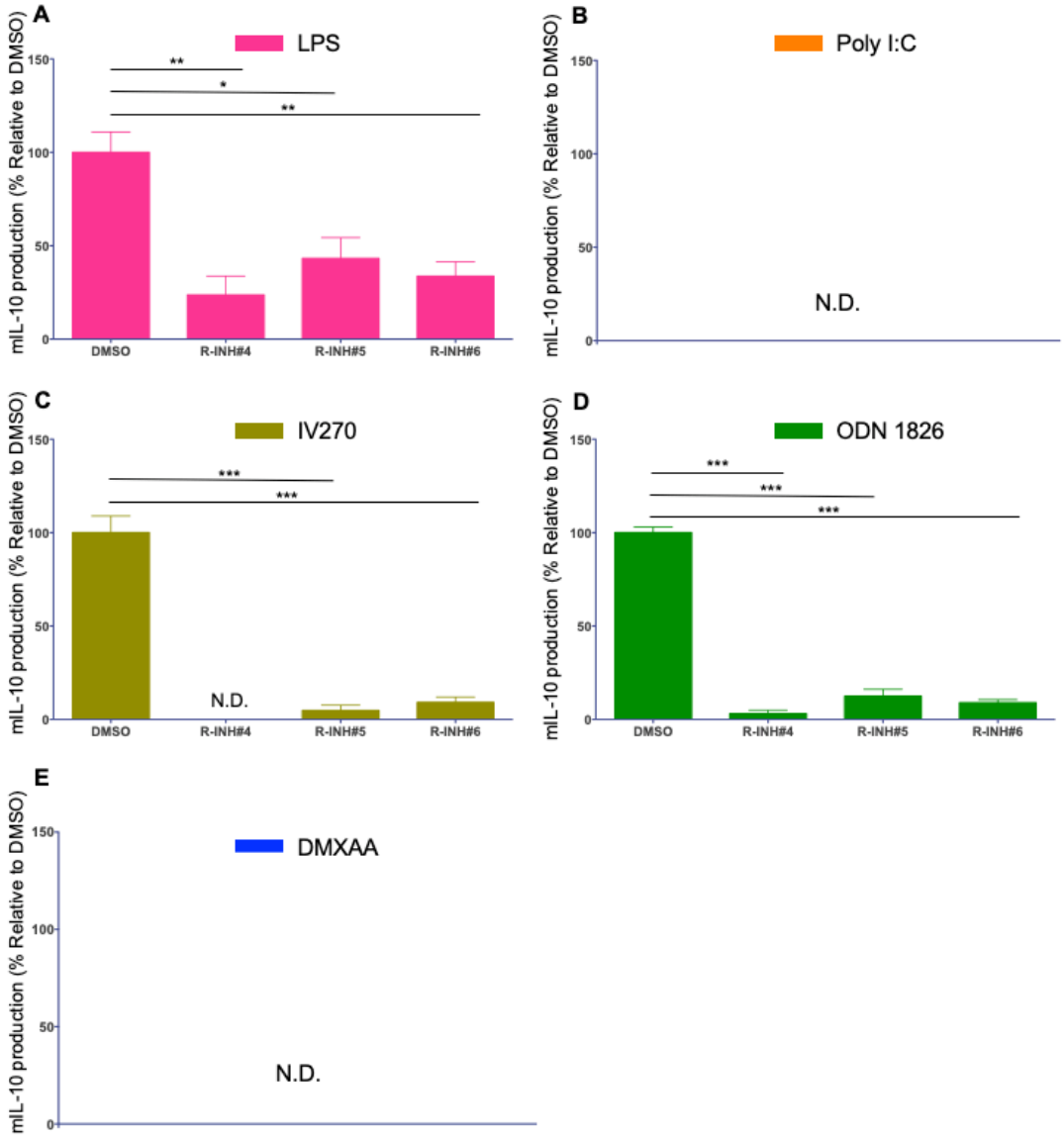

Figure 14. Relative mIL-10 expression in WT BMDCs following treatment of cells with agonists and R-INH#4-6. (A) mIL-10 levels relative to the DMSO control of BMCDs treated with LPS and respective treatments. (B) mIL-10 levels relative to the DMSO control of BMCDs treated with Poly I:C and respective treatments. (C) mIL-10 levels relative to the DMSO control of BMCDs treated with IV270 and respective treatments. (D) mIL-10 levels relative to the DMSO control of BMCDs treated with ODN 1826 and respective treatments. (E) mIL-10 levels relative to the DMSO control of BMCDs treated with DMXAA and respective treatments. Data are represented as mean ± SEM and * indicates $p < 0.05$, **$p < 0.01$, ***$p < 0.001$. N.S. – not significant. N.D. – not detected.

Table 5. Heatmap comparison of relative effects on cytokines produced when treated with respective ligands and R-INH#4-6.

R-INH#	Cytokine	TLR3-L	TLR4-L	TLR7-L	TLR9-L	STING-L
DMSO	TNFα	N.D.				
	IFNβ					
	IP10					
	IL-6					
	IL-10	N.D.				N.D.
4	TNFα	N.D.				
	IFNβ					
	IP10					
	IL-6					
	IL-10	N.D.				N.D.
5	TNFα	N.D.				
	IFNβ					
	IP10					
	IL-6					
	IL-10	N.D.				N.D.
6	TNFα	N.D.				
	IFNβ					
	IP10					
	IL-6					
	IL-10	N.D.				N.D.

3.8 Investigation of 2-Nitro Furan Arylamides as Potential STING Antagonists

Prior reports have identified other compounds of the 2-Nitro Furan Arylamide chemotype group as potential inhibitors of the STING adaptor protein (Haag et al. 2018). To assess the abilities of R-INH#4-6 in suppressing STING similar to previous reports, WT murine BMDCs were treated with DMXAA, a STING agonist, together with titrated concentrations of R-INH#4-6.

Supernatant from the treated BMDCs was extracted following an overnight incubation of the cells with agonist and compound. Following extraction, the supernatant was analyzed through a mIFNβ ELISA for relative production of mIFNβ. Treatment of STING agonist-treated BMDCs with the 2-Nitro Furan Arylamide compounds revealed an inhibition of STING-induced mIFNβ production by these candidate drugs (Figure 15A). Treatment of cells with R-INH#5 effected the greatest suppression of STING-induced mIFNβ followed by R-INH#6 and R-INH#4. Analysis of the STING-induced mIFNβ suppression was conducted to calculate the IC_{50} values of each compound (Figure 15B). IC_{50} values were found to be similar to those reported of the compounds previously identified as STING antagonists (Haag et al. 2018).

A

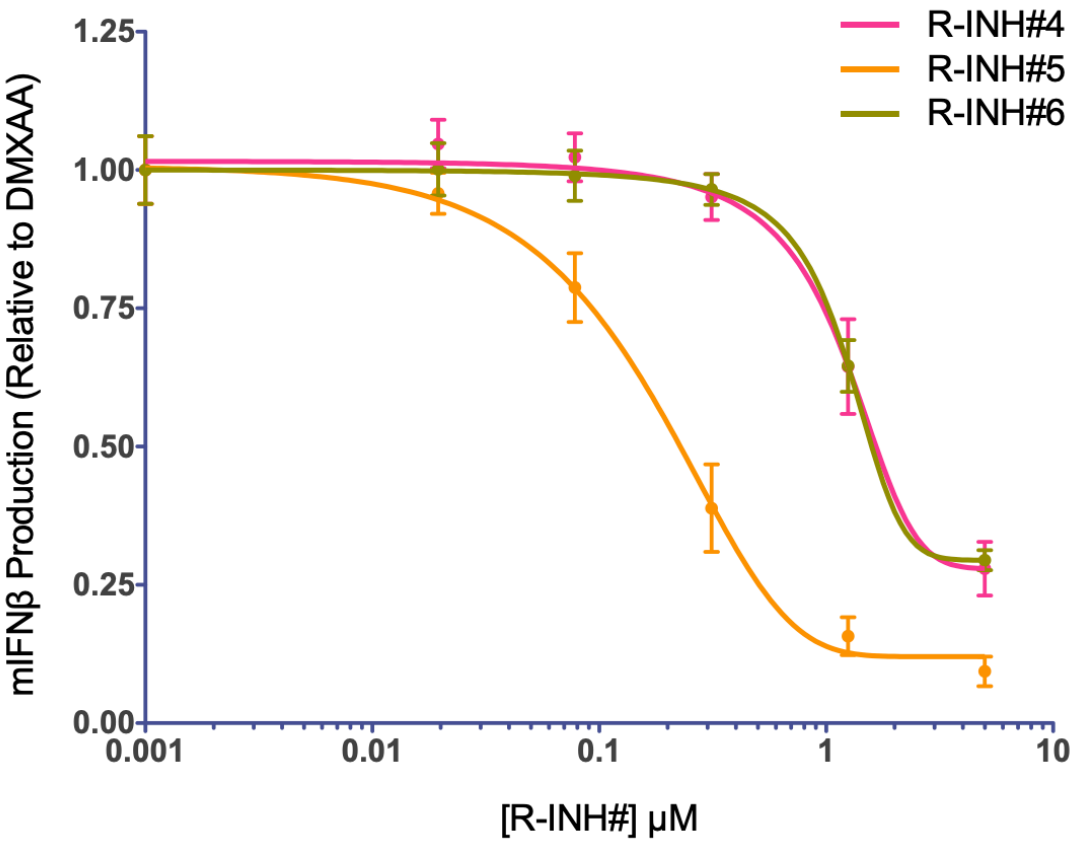

B

Compound	IC_{50}
R-INH#4	1.397 μM
R-INH#5	0.187 μM
R-INH#6	1.318 μM

Figure 15. Suppression of STING-induced mIFNβ with 2-Nitro Furan Arylamides. (A) BMDCs from WT mice were incubated with 10 μg/mL of DMXAA and titrated concentrations of R-INH#4-6 overnight and supernatant was analyzed through a mIFNβ ELISA. Data shown as mean ± SD (Compound concentration 0.001-5μM) (n=6 biological replicates). (B) IC_{50} values of R-INH#4-6.

3.9 Treatment of K/BxN Murine Arthritic Model with R-INH#5 and R-INH#6

Previous studies conducted in our lab have revealed that a reduction in TNFα and an upregulation in IFNβ can result in the resolution of neuropathic pain caused by K/BxN-induced rheumatoid arthritis (Woller et al. 2018). We conducted experiments in a K/BxN murine arthritis model to evaluate the effects of the R-INH compounds on neuropathic pain in arthritis. From the previous assays to determine the effect of these compounds with STING and other TLR pathways, we saw that R-INH#5 strongly suppressed TNFα when stimulated with various ligands and upregulated IFNβ when stimulated by LPS. Based on the compound's properties and its similarities to our previous anti-TNFα and IFNβ data in allodynia, R-INH#5 was evaluated for its effects on allodynia in the K/BxN passive serum transfer mouse model.

In a single experiment, eight male WT C57BL/6 mice were administered with K/BxN arthritic sera through intraperitoneal injection on D0 and D2 of the D28 experiment (Figure 16A). R-INH#5 was resynthesized in our lab and prepared in a DMSO stock. Mice were split into two treatment groups of three mice treated with compound and one vehicle mouse treated with DMSO alone (Figure 16B). To observe R-INH#5's preventative effects on RA, the first treatment group was treated from D0 to D5 with 750nmols of the compound administered twice daily through IP injection. Daily von Frey testing revealed that levels of allodynia in the treated mice were less than the vehicle treated mouse (Figure 17A). Furthermore, level of allodynia following the end of the treatment remained higher than the vehicle treated mouse.

To observe the effect of R-INH#5 in the recovery of existing pain in established arthritis, the second group of mice was treated with the compound twice daily from D10 to D15 once the mice expressed peak levels of allodynia. Treatment of the mice effected a mild attenuation of allodynia when compared to the vehicle that persisted following end of treatment (Figure 17B).

Together with the evaluation of allodynia of these mice, levels of ankle swelling from RA were also measured. Comparison with the DMSO-treated mice indicated that administration of R-INH#6 did not result in a difference in ankle swelling in both treatment groups (Figure 17C, D). These results show that treatment with compound alone was insufficient in effecting a reduction in arthritic swelling and was only involved in modulation of allodynia.

Once the effects of R-INH#5 were evaluated in a K/BxN model, another compound was chosen to compare the effects between the compounds. Based on commercial availability, R-INH#6 was chosen as the treatment compound to determine the effects of these drugs on RA. Another group of eight WT male mice were treated in the same manner as the initial R-INH#5. Similar to the treatment with R-INH#5, administration of R-INH#6 led to less development of allodynia at the onset of arthritis (Figure 18A). It also attenuated allodynia when mice with existing pain were treated (Figure 18B). These effects were also seen to continue to a certain extent following withdrawal of the compound treatment. However, similar to R-INH#5, no differences were observed in the swelling characteristics in both groups treated with R-INH#6 (Figure 18 C, D).

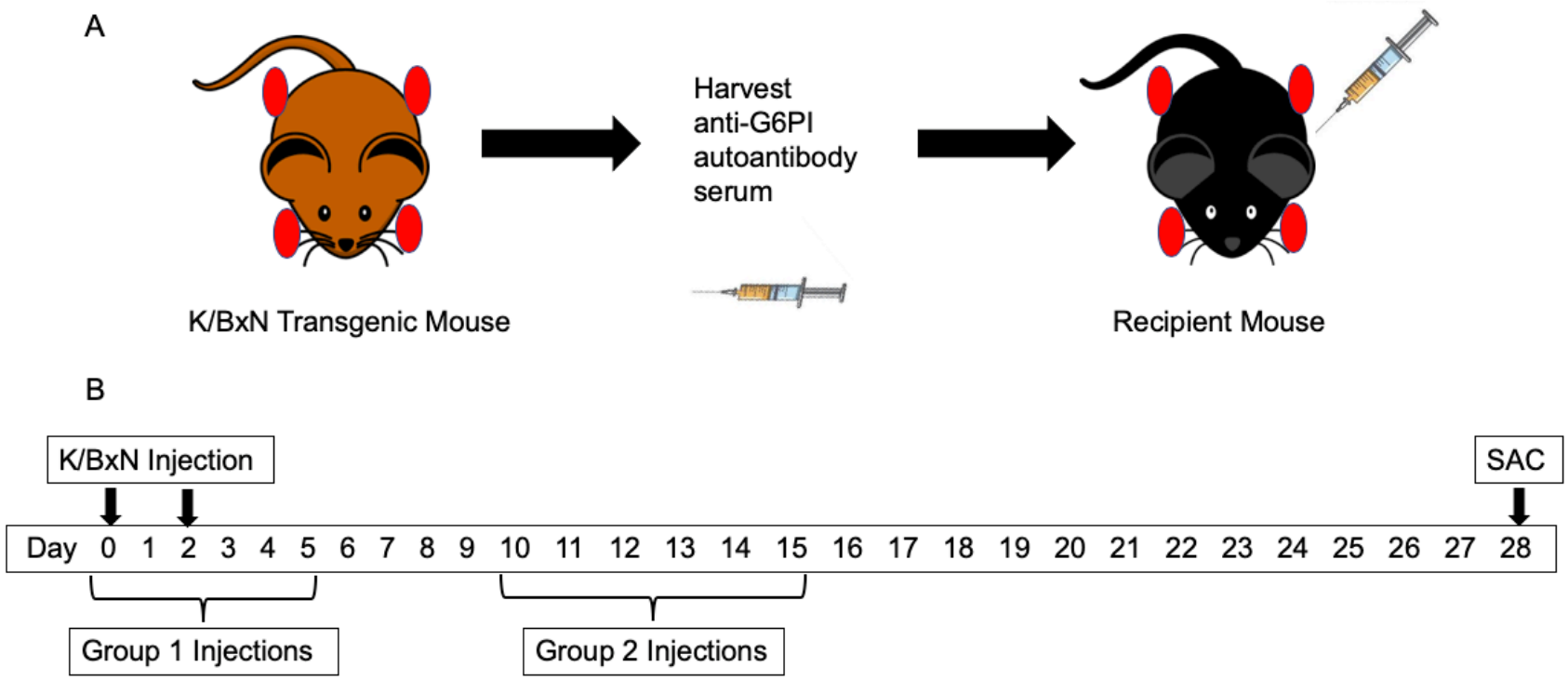

Figure 16. K/BxN murine model of arthritis and compound treatment timeline. (A) Anti-GPI autoantibody sera is extracted from K/BxN Transgenic Mice and then injected into recipient mice to induce RA. (B) Timeline of compound administration of mice for the two treatment groups.

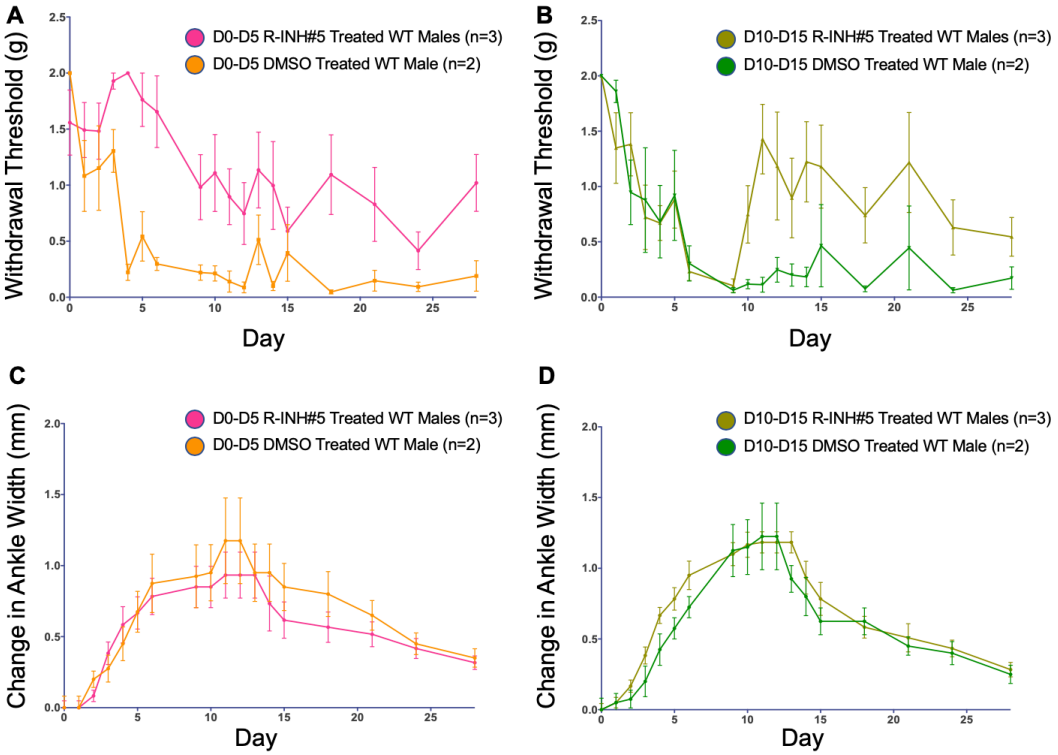

Figure 17. R-INH#5 treatment at onset of arthritis reduces development of allodynia and attenuates existing pain. (A) WT males (n = 3) were injected on days 0 and 2 with K/BxN sera and were treated twice daily from D0-D5 with R-INH#6. Tactile allodynia in mice treated with R-INH#6 is less severe than control treated with DMSO. Data are represented as mean ± SEM. (B) WT males (n=3) were treated from D10-D15 with R-INH#6. Mild attenuation of allodynia in compound-treated mice. (C, D) Measurements of ankle swelling in both treatment groups indicate that administration of R-INH#6 does not affect swelling caused by arthritis.

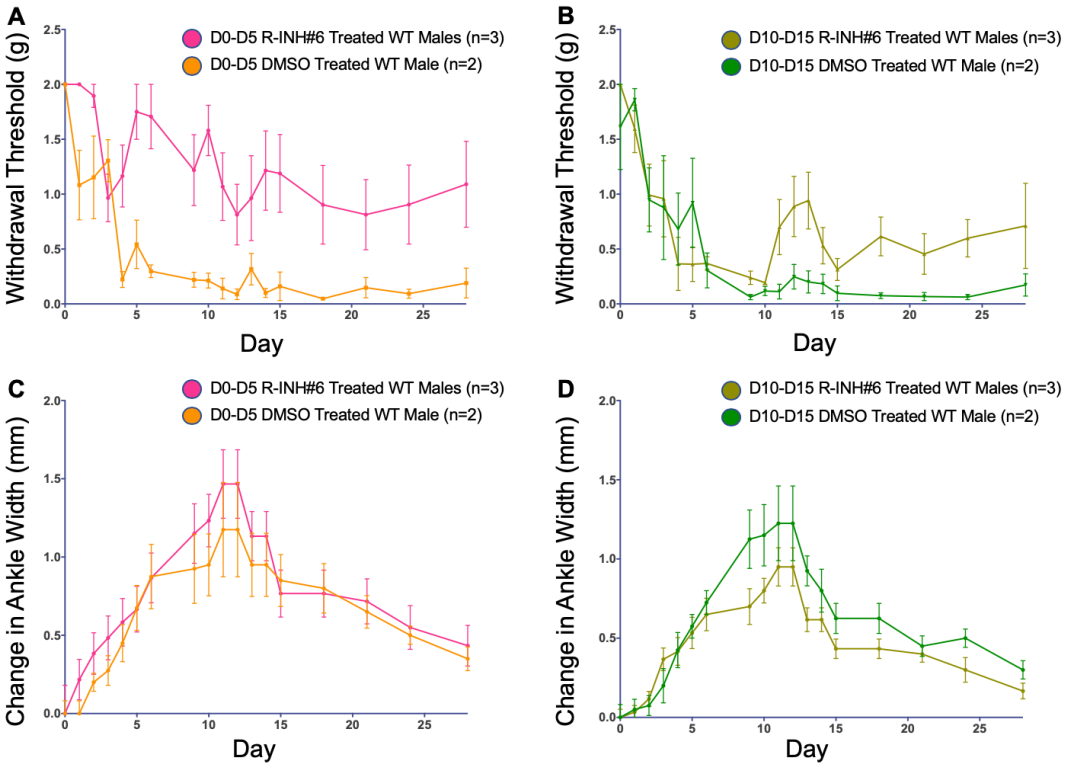

Figure 17. R-INH#6 treatment at onset of arthritis reduces development of allodynia and attenuates existing pain. (A) WT males (n = 3) were injected on days 0 and 2 with K/BxN sera and were treated twice daily from D0-D5 with R-INH#6. Tactile allodynia in mice treated with R-iNH#6 is less severe than control treated with DMSO. Data are represented as mean ± SEM. (B) WT males (n=3) were treated from D10-D15 with R-INH#6. Mild attenuation of allodynia in compound-treated mice. (C, D) Measurements of ankle swelling in both treatment groups indicate that administration of R-INH#6 does not affect swelling caused by arthritis.

4. Discussion

To identify potential immunomodulators that could cause a decrease in pro-inflammatory cytokines associated with TLR pathways, we conducted an HTS to analyze a compound library for suppression of NF-κB. From the HTS, we were able to identify 1824 compounds with activity similar to known glucocorticoids for downregulation of LPS-induced NF-κB activation for further assessment. These compounds were picked from the region of data where known glucocorticoids, that were included in the chemical library of the main screen, showed activity. From the 166,304 compounds in the main screen, 1,843 compounds were picked for the secondary screening. The number of compounds equates to an approximate 1.1% of compounds selected from the main HTS for future validation tests. Oprea reports that single-dose HTS, where compounds are tested in singlets, typically show a success rate of below 0.1% (Oprea 2002). It is also noted that a portion of the 0.1% selection group includes false positives that appear in HTS readouts (Oprea 2002). Our confirmation screen yielded that 14.6% of compounds were reproducible which is indicative of the high effectiveness of our selection method of using known immunosuppressant data regions to identify candidate targets.

Once these 1843 compounds were reassessed for their suppression of LPS-induced NF-κB activation at two different timepoints following compound incubation, another smaller compound set was selected for further validation based mainly on a Top X selection approach (Pu et al. 2013). Some variability existed in this screening as some compounds did not fit the predetermined Top X parameters for both data points after being run in duplicate. A total of 270

compounds were identified from the confirmation screening of 1,824 selected compounds, equating to an approximate 15% reproducibility rate. This is a relatively high number as typically 50-200 compounds are identified from about 2000 compounds in normal HTS which corresponds to a 2.5-10% selection efficiency (Hann et al., 2004). The higher selection rate we had is likely due to having a higher proportion of potential candidates in the secondary screening following identification of compounds closely associated with glucocorticoid activity in the first round of selection. The use of the Top X approach to set screening parameters has been criticized for its selection efficiency and low confirmation rate (Yan et al., 2005). However, the use of parameters set around the activity of known glucocorticoids in the first round of selection lead to better efficiency by focusing attention to compounds in data regions containing established immunosuppressants similar to those we were trying to identify.

Yan and colleagues suggest that employment of SAR (structural activity relationship) analysis in early stages of screening can be useful in identifying potential compounds which can be later optimized for better activity based on its chemical structure (Yan et al. 2005). SAR analysis is conducted by analyzing the structures of chemical compounds to determine their effects on biology as some structures are more suited to effect certain physiological responses than others. In our screening, we did not use SAR as a selection basis in early screening due to high volume of compounds and variability in suppression of NF-κB activation among chemicals having similar chemotypes (chemical structures). Instead, we used SAR as a basis from which to pick compounds at

later stages within the screening process on a smaller pool of candidate compounds.

Analysis of the compounds for relative cytokine production and cytotoxicity revealed that compounds which produced high levels of IL-8 also had high relative toxicity in treated cells. This served as a reliable marker to determine the potential use of the compounds. However, subsequent screening of compounds which met set requirement thresholds involved the elimination of certain chemotypes which had issues based on their chemical structure, such as being Michael acceptors. Screening may have been more efficient with the removal of these compounds from the candidate pool at earlier stages of the screening.

Following purchasing of the R-INH# series, we saw that only half of the compounds were able to replicate their cytokine production behavior from the initial screening. Analysis of the R-INH# compounds and the original compounds through mass spectrometry revealed that several of the original compounds had degraded over time and was the likely cause for the disparity in the results. Further analysis in the murine RAW cell line showed that only several of the R-INH# series was able to maintain similar behavior in a murine model. However, to meet the end goal of eventual use in human disease following assessment in mice, it was important to select compounds which were functional in both human and murine cell types.

Further testing revealed 2-Nitrofuran Arylamides as the lead chemotype group. Comparison to previously reported compounds shows that there is high possibility of these compounds could function through the STING complex.

Dual treatment with the compounds and a STING agonist in WT murine BMDCs showed an inhibition of the response of IFNβ when treated with R-INH#4. We saw that R-INH#5 had the greatest inhibition effect followed by R-INH#6 and R-INH#4, respectively. This was consistent with the respective inhibition of TNFα that was observed in treatment of compounds with LPS stimulation in RAW cells.

In previous literature of compounds from this chemotype group, it was shown that treatment of these compounds with CpG stimulation resulted in a suppression of IFNβ but not with stimulation by LPS. Assessment of the relative inhibition of cytokines revealed that the compounds caused inhibition of various cytokines when treated by TLR3, TLR-4, TLR-7, and TLR-9 ligands in addition to STING ligands. Of note, treatment of R-INH#5 with LPS stimulation resulted in an upregulation of the levels of IFNβ. This is indicative that the compounds are not specific to STING and in fact work through various pathways. The lack of specificity of these small-molecule compounds suggests that investigation of a multitude of pathways is necessary to understand the effects of these compounds.

Due to the murine specificity of the DMXAA agonist, we could not determine whether the results were replicable in human models. Further evaluation through use of human STING agonists would serve to assess the behavior of these compounds in a human model. It was shown that of the three compounds from the 2-nitrofuran arylamide chemotype that were studied, R-INH#4 was most effective in human cells but not in murine cells. Analysis of the compounds in a human cell model may reveal different degrees of behavior

between the compounds. We expect that R-INH#4 may have higher levels of suppression when used in human-derived primary cell lines. However, complexes like STING must be carefully considered due to polymorphic differences between individuals of the same species.

In the K/BxN murine model of arthritis, we observed that there is a strong interrelationship between TLR pathway activity and the development and progression of pain. Pathogenesis of the disease was shown to be affected by various cytokines associated with innate immune pathways. Comparison of WT mice of both sexes showed that males experienced persistent pain following resolution of swelling while females showed attenuation of pain. However, investigation of *Tlr4*$^{-/-}$ mice with arthritis revealed that both sexes of this strain resolved their pain over time and females showed consistently better resolution of swelling.

To determine causes for attenuation of allodynia, expression of TLR4-associated cytokines was assessed to understand their role in pain. Ten days following administration of K/BxN serum, *Tnf* expression levels were seen to be reduced in *Tlr4*$^{-/-}$ males compared to WT males and *Ifnb1* levels were increased in both *Tlr4*$^{-/-}$ males and females. Translation of these findings to administer both TNF-antibodies and IFN IT to WT mice with arthritis effected an attenuation of pain which persisted after administration of treatment (Woller et al. 2018).

To assess whether these compounds would be useful as a pain treatment for arthritis, we first treated mice with R-INH#5 which exhibited a strong inhibition of TNFα and upregulated IFNβ with LPS stimulation. Through

administration of R-INH#5 in a K/BxN model, a general trend of allodynia being suppressed following treatment at the beginning of the experiment was observed. A transient increase of mechanical sensitivity was also seen following administration of the second dose of K/BxN sera but was resolved with treatment. Allodynia did increase once compound administration was ended, but allodynia did not reach similar levels as that of the vehicle mouse. Treatment with compound following maximum expression of allodynia mildly attenuated allodynia which continued after end of compound administration. However, swelling was not affected by administration of these drugs. This was an expected outcome as we saw that these drugs suppressed levels of IL-10, an anti-inflammatory cytokine. These results indicated that a dual treatment of R-INH#5 with another compound may serve to effect remission of both allodynia and swelling.

Assessment of mechanical sensitivity was subsequently redone with R-INH#6 and similar results to the previous R-INH#5 treatment experiment was observed. The similarities between the two compounds indicate that R-INH#5's ability to upregulate IFNβ with LPS stimulation is not the only factor that is responsible for the attenuation of allodynia. It is likely that there are other factors involved which are responsible for the resolution of allodynia.

This thesis, in part, is currently being prepared for submission for publication of the material. Fujita, Yuya; Hosoya, Tadashi; Shukla, Nikunj; Cottam, Howard; Hayashi, Tomoko; Carson, Dennis; Corr, Mary P. The thesis author was the primary investigator and author of this material.

References

Bajar, Bryce T, Emily S Wang, Shu Zhang, Michael Z Lin, and Jun Chu. 2016. "A Guide to Fluorescent Protein FRET Pairs." *Sensors* 16 (2): 1–24. https://doi.org/10.3390/s16091488.

Beutler, Bruce A. 2019. "Review Article TLRs and Innate Immunity." *Blood Journal* 113 (7): 1399–1408. https://doi.org/10.1182/blood-2008-07-019307.

Borenstein, David, Roy Altman, Alfonso Bello, Winn Chatham, Daniel Clauw, Leslie Crofford, Joseph Croft, Afton Hasset, Franklin Kozin, David Pisetsky, Jan Richardson, Laura Schanberg, Terence Starz, and James Witter. 2010. "Report of the American College of Rheumatology Pain Management Task Force." *Arthritis Care and Research* 62 (5): 590–99. https://doi.org/10.1002/acr.20005.

Burmester, Gerd R., and Janet E. Pope. 2017. "Novel Treatment Strategies in Rheumatoid Arthritis." *The Lancet* 389 (10086): 2338–48. https://doi.org/10.1016/S0140-6736(17)31491-5.

Chan, Michael, Alast Ahmadi, Shiyin Yao, Fumi Sato-Kaneko, Karen Messer, Minya Pu, Brandon Nguyen, Tomoko Hayashi, Maripat Corr, Dennis A Carson, Howard B Cottam, and Nikunj M Shukla. 2017. "Identification of Biologically Active Pyrimido[5, 4-b]Indoles That Prolong NF-KB Activation without Intrinsic Activity." *ACS Combinatorial Science* 19 (8): 533–43. https://doi.org/10.1021/acscombsci.7b00080.

Chang, Kathleen, So Min Yang, Seong Heon Kim, Kyoung Hee Han, and Se Jin Park. 2014. "Smoking and Rheumatoid Arthritis." *International Journal of Molecular Sciences* 15: 22279–95. https://doi.org/10.3390/ijms151222279.

Chaplan, SR, Bach, FW, Pogrel, JW, Chung, JM, Yaksh, TL. 1994. "Quantitative Assessment of Tactile Allodynia Evoked by Unilateral Ligation of the Fifth and Sixth Lumbar Nerves in the Rat." *Journal of Neuroscience* 53: 55–63.

Christianson, Christina A., Maripat Corr, Gary S Firestein, Anahita Mobargha, Tony L Yaksh, and Camilla I Svensson. 2010. "Characterization of the Acute and Persistent Pain State Present in K/BxN Serum Transfer Arthritis." *Drugs* 151 (2): 1311–20. https://doi.org/10.1016/j.pain.2010.07.030.Characterization.

Christianson, Christina a, Maripat Corr, Tony L Yaksh, and Camilla I Svensson. 2012. "K/BxN Serum Transfer Arthritis as a Model of Inflammatory Joint Pain." *Methods Mol Biol.* 851: 249–60. https://doi.org/10.1111/j.1526-

4610.1973.hed1303131.x.

Corr, M, D L Boyle, L Ronacher, N Flores, and G S Firestein. 2009. “Synergistic Benefit in Inflammatory Arthritis by Targeting IκB Kinase ε and Interferon β.” *Ann Rheum Dis* 68 (2): 257–63. https://doi.org/10.1136/ard.2008.095356.Synergistic.

Corr, M, D Boyle, L Ronacher, B Lew, L Van Baarsen, P Tak, and G Firestein. 2011. “Interleukin 1 Receptor Antagonist Mediates the Beneficial Effects of Systemic Interferon Beta in Mice: Implications for Rheumatoid Arthritis.” *Annals of the Rheumatic Diseases* 70 (5): 858–63.

Curtis, Jeffrey R., and Jasvinder A. Singh. 2013. “The Use of Biologics in Rheumatoid Arthritis: Current and Emerging Paradigms of Care.” *Clinical Therapeutics* 33 (6): 679–707. https://doi.org/10.1016/j.clinthera.2011.05.044.The.

Datta, Sandip K, Vanessa Redecke, Kiley R Prilliman, Maripat Corr, Thomas Tallant, Roman Dziarski, Shizuo Akira, and P Stephen. 2003. “A Subset of Toll-Like Receptor Ligands Induces Cross-Presentation by Bone Marrow-Derived Dendritic Cells.” *The Journal of Immunology* 170 (8): 4102–10. https://doi.org/10.4049/jimmunol.170.8.4102.

Endo, Tomoyuki, Mitsufumi Nishio, Thomas Enzler, Howard B Cottam, Tetsuya Fukuda, F Danelle, Michael Karin, Thomas J Kipps, Washington Dc, and Danelle F James. 2012. “BAFF and APRIL Support Chronic Lymphocytic Leukemia B-Cell Survival through Activation of the Canonical NF- κ B Pathway BAFF and APRIL Support Chronic Lymphocytic Leukemia B-Cell Survival through Activation of the Canonical NF- B Pathway” 109 (2): 703–10. https://doi.org/10.1182/blood-2006-06-027755.

González-Navajas, José M., Jongdae Lee, Michael David, and Eyal Raz. 2012. “Immunomodulatory Functions of Type i Interferons.” *Nature Reviews Immunology* 12 (2): 125–35. https://doi.org/10.1038/nri3133.

Haag, Simone M., Muhammet F. Gulen, Luc Reymond, Antoine Gibelin, Laurence Abrami, Alexiane Decout, Michael Heymann, F. Gisou van der Goot, Gerardo Turcatti, Rayk Behrendt, and Andrea Ablasser. 2018. “Targeting STING with Covalent Small-Molecule Inhibitors.” *Nature* 559 (7713): 269–73. https://doi.org/10.1038/s41586-018-0287-8.

Hann, Mike M, and Tudor I Oprea. 2004. “Pursuing the Leadlikeness Concept in Pharmaceutical Research.” *Current Opinion in Chemical Biology* 8: 255–63. https://doi.org/10.1016/j.cbpa.2004.04.003.

Holten, Judith van, Christine Plater-Zyberk, and Paul P. Tak. 2002. “Interferon-β for Treatment of Rheumatoid Arthritis?” *Arthritis Research* 4 (6): 346–52.

https://doi.org/10.1186/ar598.

Kawasaki, Takumi, and Taro Kawai. 2014. “Toll-like Receptor Signaling Pathways.” *Frontiers in Immunology* 5 (September): 1–8. https://doi.org/10.3389/fimmu.2014.00461.

Kouskoff, Vale´rie, Anne-Sophie Korganow, Ve´ronique Duchatelle, Claude Degott, Christophe Benoist, Diane Mathis, and Illkirch Cedex. 1996. “Organ-Specific Disease Provoked by Systemic Autoimmunity.” *Cell* 87: 811–22.

Lee, David M, and Michael E Weinblatt. 2001. “Rheumatoid Arthritis.” *The Lancet* 358 (9285): 903–11. https://doi.org/10.1016/S0140-6736(01)06075-5.

Lee, Suki Man-yan, Tsz-fung Yip, Sheng Yan, Dong-yan Jin, Hong-li Wei, Amanda Jane Gibson, and Suki Man-yan Lee. 2018. “Recognition of Double-Stranded RNA and Regulation of Interferon Pathway by Toll-Like Receptor 10.” *Frontiers in Immunology* 9 (March). https://doi.org/10.3389/fimmu.2018.00516.

Li, Yang, Heather L Wilson, and Endre Kiss-toth. 2017. “Regulating STING in Health and Disease.” *Journal of Inflammation* 14 (11): 1–21. https://doi.org/10.1186/s12950-017-0159-2.

Liu, Ting, Lingyun Zhang, Donghyun Joo, and Shao-Cong Sun. 2017. “NF-KB Signaling in Inflammation.” *Signal Transduction and Targeted Therapy* 2 (April): 17023. https://doi.org/10.1038/sigtrans.2017.23.

Liu, Yin, Adriana A Jesus, Bernadette Marrero, Dan Yang, Suzanne E Ramsey, Gina A Montealegre Sanchez, Klaus Tenbrock, Helmut Wittkowsi, Olcay Y Jones, Hye Sun Kuehn, Chyi-Chia R Lee, Michael A DiMattia, Edward W Cowen, Benito Gonzalez, Ira Palmer, John J DiGiovanna, Angelique Biancotto, Hanna Kim, Wanxia L Tsai, Anna M Trier, Yan Huang, Deborah L Stone, Suvimol Hill, H. Jeffery Kim, Cynthia St. Hilaire, Shakuntala Gurprasad, Nicole Plass, Dawn Chapelle, Iren Horkayne-Szakaly, Dirk Foell, Andrei Barysenka, Fabio Candotti, Steven M Holland, Jason D Hughes, Huseyin Mehmet, Andrew C Issekutz, mark Raffeld, Joshua McElwee, Joseph R Fontana, Caterina P Minniti, Susan Moir, Daniel L Kastner, Massimo Gadina, Alasdair C Steven, Paul T Wingfield, Stephen R Brooks, Sergio D Rosenzweig, Thomas A Fleisher, Zuoming Deng, Manfred Boehm, Amy S Paller, and Raphaela Golbach-Mansky. 2014. “Activated STING in a Vascular and Pulmonary Syndrome.” *The New England Journal of Medicine*, 507–18. https://doi.org/10.1056/NEJMoa1312625.

Matsumoto, Isao, and Adrien Staub. 1999. “Arthritis Provoked by Linked T and

B Cell Recognition of a Glycolytic Enzyme." *Science* 286 (5445): 1732–35. https://doi.org/10.1126/science.286.5445.1732.

Mcnab, Finlay, Katrin Mayer-barber, Alan Sher, Andreas Wack, and Anne O Garra. 2015. "Type I Interferons in Infectious Disease." *Nature Publishing Group* 15 (2): 87–103. https://doi.org/10.1038/nri3787.

Minnock, Patricia, Douglas J. Veale, Barry Bresnihan, Oliver FitzGerald, and Gabrielle McKee. 2015. "Factors That Influence Fatigue Status in Patients with Severe Rheumatoid Arthritis (RA) and Good Disease Outcome Following 6 Months of TNF Inhibitor Therapy: A Comparative Analysis." *Clinical Rheumatology* 34 (11): 1857–65. https://doi.org/10.1007/s10067-015-3088-6.

Miyawaki, Atsushi. 2011. "Development of Probes for Cellular Functions Using Fluorescent Proteins and Fluorescence Resonance Energy Transfer." *Annual Review of Biochemistry* 80: 357–73. https://doi.org/10.1146/annurev-biochem-072909-094736.

Murphy, Louise B., Jeffrey J. Sacks, Teresa J. Brady, Jennifer M. Hootman, and Daniel P. Chapman. 2012. "Anxiety and Depression among US Adults with Arthritis: Prevalence and Correlates." *Arthritis Care and Research* 64 (7): 968–76. https://doi.org/10.1002/acr.21685.

Oprea, Tudor I. 2002. "Current Trends in Lead Discovery : Are We Looking for the Appropriate Properties ?," 325–34.

Podolin, Patricia L, James F Callahan, Brian J Bolognese, Yue H Li, Karey Carlson, T Gregg Davis, Geoff W Mellor, Christopher Evans, and Amy K Roshak. 2005. "Attenuation of Murine Collagen-Induced Arthritis by a Novel , Potent , Selective Small Molecule Inhibitor of I B Kinase 2 , Thiophenecarboxamide), Occurs via Reduction of Proinflammatory Cytokines and Antigen-Induced T Cell Proliferation." *The Journal of Pharmacology and Experimental Therapeutics* 312 (1): 373–81. https://doi.org/10.1124/jpet.104.074484.characterizes.

Pu, Minya, Tomoko Hayashi, Howard Cottam, Joseph Mulvaney, Michelle Arkin, Maripat Corr, Dennis Carson, and Karen Messer. 2013. "Analysis of High Throughput Screening Assays Using Cluster Enrichment." *Stat Med* 31 (30): 4175–89. https://doi.org/10.1002/sim.5455.Analysis.

Scott, David L, Frederick Wolfe, and Tom W J Huizinga. 2010. "Rheumatoid Arthritis." *The Lancet* 376 (9746): 1094–1108. https://doi.org/10.1016/S0140-6736(10)60826-4.

Smolen, Josef S, Daniel Aletaha, Anne Barton, Gerd R Burmester, Paul Emery, Gary S Firestein, Arthur Kavanaugh, Ian B McInnes, Daniel H Solomon,

Vibeke Strand, and Kazuhiko Yamamoto. 2018. “Rheumatoid Arthritis.” *Nature Publishing Group* 4: 1–23. https://doi.org/10.1038/nrdp.2018.1.

Vaure, Céline, and Yuanqing Liu. 2014. “A Comparative Review of Toll-like Receptor 4 Expression and Functionality in Different Animal Species.” *Frontiers in Immunology* 5 (July): 1–15. https://doi.org/10.3389/fimmu.2014.00316.

Wilsdon, Tom D, and Catherine L Hill. 2017. “Managing the Drug Treatment of Rheumatoid Arthritis.” *Australian Prescriber* 40 (2): 51–58. http://dx.doi.org/10.18773/%0Aaustprescr.2017.012.

Woller, Sarah A, Cody Ocheltree, Stephanie Y Wong, Anthony Bui, Yuya Fujita, Gilson Goncalves dos Santos, Tony L Yaksh, and Maripat Corr. 2018. “Brain , Behavior , and Immunity Neuraxial TNF and IFN-Beta Co-Modulate Persistent Allodynia in Arthritic Mice.” *Brain Behavior and Immunity*, no. June: 0–1. https://doi.org/10.1016/j.bbi.2018.11.014.

Yan, S Frank, Hayk Asatryan, Jing Li, and Yingyao Zhou. 2005. “Novel Statistical Approach for Primary High-Throughput Screening Hit Selection,” 1784–90. https://doi.org/10.1021/ci0502808.

Yeap, S S, and D J Hosking. 2002. “Management of Corticosteroid-Induced Osteoporosis.” *Rheumatology* 41: 1088–94.